Quaternary Science Reviews 29 (2010) 2647–2662

Contents lists available at ScienceDirect

Quaternary Science Reviews

journal homepage: www.elsevier.com/locate/quascirev

Middle-Late Quaternary paleoclimate of northern margins of the Saharan-Arabian Desert: reconstruction from speleothems of Negev Desert, Israel

Anton Vaks [a,b,c,*], Miryam Bar-Matthews [b], Alan Matthews [c], Avner Ayalon [b], Amos Frumkin [d]

[a] Department of Earth Sciences, University of Oxford, Parks Road, Oxford OX1 3PR, UK
[b] Geological Survey of Israel, 30 Malchei Israel St, Jerusalem 95501, Israel
[c] Institute of Earth Sciences, Hebrew University, Jerusalem 91904, Israel
[d] Department of Geography, Hebrew University, Jerusalem 91905, Israel

ARTICLE INFO

Article history:
Received 9 September 2009
Received in revised form
17 May 2010
Accepted 9 June 2010

ABSTRACT

Speleothems in arid and hyper-arid areas of Negev Desert, Israel, are used in paleoclimate reconstruction of northern margins of Saharan-Arabian Desert, focused on the following objectives: 1) precise U–Th dating of the timing of speleothem growth as an indicator of periods of humid climate, i.e. positive effective precipitation; 2) the origin of rainfall using the speleothem $\delta^{18}O$ and changes in spatial pattern of speleothem deposition and speleothem thickness along a north–south transect; 3) changes of vegetation cover based on speleothem $\delta^{13}C$ variations.

During the last 350 ka major humid periods, referred to herein as Negev Humid Periods (NHP), occurred in the central and southern Negev Desert at 350–310 ka (NHP-4), 310–290 ka (NHP-3), 220–190 ka (NHP-2), and 142–109 ka (NHP-1). NHP-4, NHP-2 and NHP-1 are interglacial events, whereas NHP-3 is associated with a glacial period. During NHP-1, 2 and 3 the thickness and volume of the speleothems decrease from the north to the south, and in the most southern part of the region only a very thin flowstone layer formed during NHP-1, with no speleothem deposition occurring during NHP-2 and 3. These data imply that the Eastern Mediterranean Sea was the major source of the rainfall in northern and central Negev. More negative speleothem $\delta^{18}O$ values, relative to central parts of Israel (Soreq Cave) are attributed to Rayleigh distillation because of the increasing distance from the Mediterranean Sea. Speleothem deposition during the NHP-4 in the southern Negev was more intensive than in most of the central Negev, suggesting the prominence of the tropical rain source.

Decrease in speleothem $\delta^{13}C$ during NHP events indicates growth of the vegetation cover. Nevertheless, the ranges of $\delta^{13}C$ values show that the vegetation remained semi-desert C4 type throughout the NHPs, with an additional significant carbon fraction coming from the host rock and the atmosphere. These observations, together with small thickness of the speleothem layers, favor that NHP events consisted of clusters of very short humid episodes interspersed with long droughts.

NHP events were contemporaneous with climate periods with monsoon index of ≥ 51 (cal/cm^2 × day) and with the formation of sapropel layers in the Mediterranean Sea. Such simultaneous intensification of the monsoon and Atlantic-Mediterranean cyclones is probably related to the weakening of the high pressure cell above sub-tropical Atlantic Ocean, which enabled more rainfall to penetrate into the Saharan-Arabian Desert from the north and south. The contemporaneous occurrence of the NHP events and the increased monsoon rainfall could have opened migration corridors, creating climatic "windows of opportunity" for dispersals of hominids and animals out of the African continent.

1. Introduction

The Saharan-Arabian Desert (Fig. 1A) is the largest and the most arid desert in the world, but its climatic history is punctuated by many humid periods since its formation ~2.7 Ma ago (deMenocal, 1995, 2004). The Quaternary paleoclimate of southern and central part of Saharan-Arabian Desert was strongly related to monsoon activity, which increased during periods of maximum northern hemisphere insolation, leading to the formation of lakes and rivers in these present-day hyper-arid region (Street and Grove, 1979; Szabo et al., 1995; Crombie et al., 1997; Rohling et al., 2002;

* Corresponding author. Tel.: +44 18652 82154; fax: +44 18652 72072.
E-mail address: Anton.Vaks@earth.ox.ac.uk (A. Vaks).

0277-3791/$ – see front matter © 2010 Elsevier Ltd. All rights reserved.
doi:10.1016/j.quascirev.2010.06.014

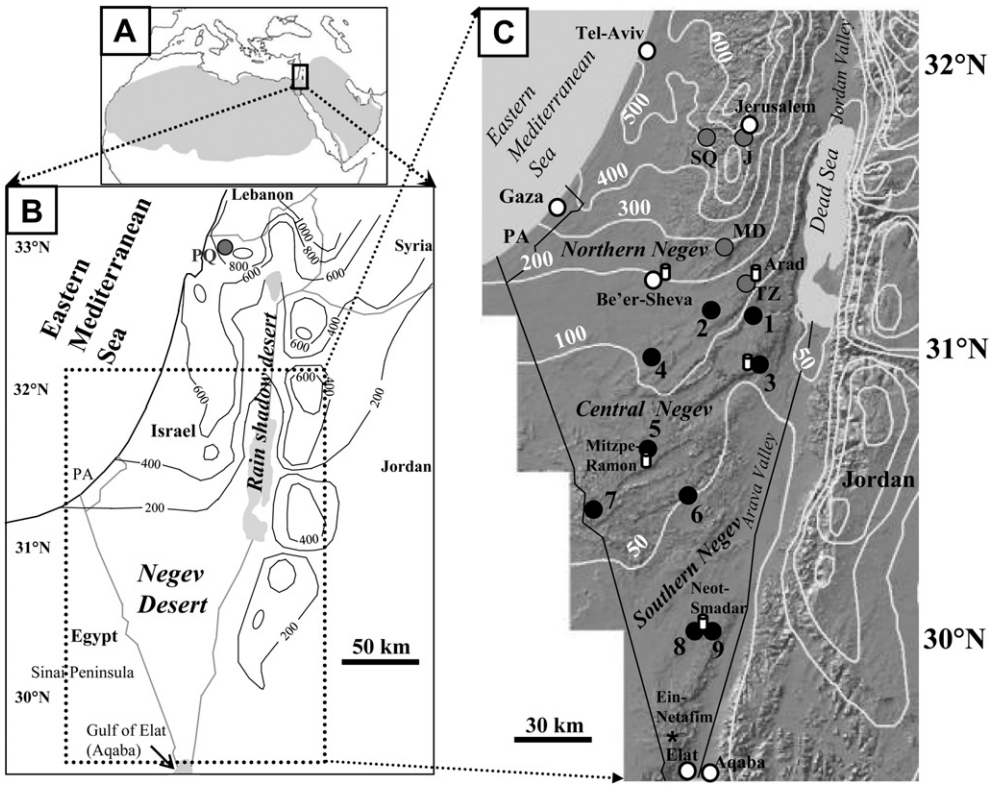

Fig. 1. Geographical location of the study area, annual precipitation and sample sites. (A) Map indicating the extent of the Saharan-Arabian Desert (shaded grey area). The rectangle marks the research area; (B) Annual rainfall map of Israel and adjacent lands: Palestinian Authority in Gaza (PA), north-eastern Egypt, western Jordan, south-western Syria, and southern Lebanon. Isohyets are indicated by black lines. Peqi'in Cave (PQ) (Bar-Matthews et al., 2003) located in northern Israel is marked. The dotted rectangle (enlargement in C) indicates the location of the desert caves studied in this research. (C) Map showing the relief (Hall, 1997), precipitation and location of the studied caves. The isohyets are marked by white lines and studied caves by black circles and numbers as following: 1 – Hol-Zakh Cave, 2 – Izzim Cave, 3 – Makhtesh-ha-Qatan Cave, 4 – Ashalim Cave, 5 – Even-Sid mini-caves, 6 – Ma'ale-ha-Meyshar Cave, 7 – Wadi-Lotz Cave; Southern Negev: 8 – Shizafon mini-caves and 9 – Ktora Cracks. Other caves from other parts of Israel that were subject for previous studies (e.g. Bar-Matthews et al., 1997, 2003; Frumkin et al., 1999; Vaks et al., 2003, 2006); are marked by grey circles and abbreviations as follows: Central Israel: SQ – Soreq Cave, J – Jerusalem Cave; Northern Negev: MD – Ma'ale-Dragot Caves; TZ – Tzavoa Cave. The rain sampling stations at Be'er-Sheva, Arad, Makhtech-ha-Qatan, Mitzpe-Ramon and Neot Smadar, are indicated by white cylinders. Ein-Netafim spring near Elat is shown by a star.

Osmond and Dabous, 2004; Osborne et al., 2008). The northern margin of Saharan-Arabian Desert receives its present-day precipitation from mid-latitude Atlantic-Mediterranean cyclones (Dayan, 1986), but the factors affecting the paleoclimate of this region are still not well understood. Wet periods in northern margin of Saharan-Arabian Desert would have been critical for the northward migration of human and animal species out of Africa through geographical corridors, such as the Sinai-Negev land bridge between Africa and Asia (Vaks et al., 2007).

Carbonate cave deposits (speleothems) potentially provide one of the most valuable paleoclimate archives in this region, because of their high dating precision and high-resolution stable isotope records. Speleothems grow in caves when water penetrates into the unsaturated zone and surface vegetation is present to supply the CO_2 necessary for limestone dissolution (Hendy, 1971; Schwarcz, 1986), but they do not grow in water and soil-CO_2 depleted conditions of arid/hyper-arid deserts (Holmgren et al., 1995; Fleitmann et al., 2003). Thus, speleothem deposition is an indication that an annual season of positive effective precipitation (i.e. precipitation – (evaporation + runoff)) has occurred above the cave. Speleothem deposition in the Mediterranean climate part of Israel was continuous during the last 240 ka, and continues in the present (Bar-Matthews et al., 2003), whereas their formation was only intermittent in the more arid regions of Israel. Recent studies on Israeli semi-desert regions, where speleothems do not grow today, reveal that high effective precipitation resulting in speleothem deposition occurred there mainly during two last glacial periods (Vaks et al., 2003, 2006; Lisker et al., 2010). Lower effective precipitation prevailed during the two last interglacials and resulted in limited speleothem deposition during minor wet episodes. However, in the arid and hyper-arid region of central and southern Negev Desert dry conditions prevailed during the two last glacial periods, and only minor wet episodes occurred during the penultimate interglacial (140–110 ka and ~88 ka) (Vaks et al., 2007).

This work presents the U–Th dating and stable isotope composition records of speleothems from caves in the arid/hyper-arid central and southern Negev Desert situated between present-day 150 mm and 30 mm isohyets, and located at northern margins of the Saharan-Arabian Desert (Fig. 1B and C). The key issues of this study is to understand the contrast between the paleoclimate of the desert and less arid region further to the north, and to expand the speleothem record in the desert beyond our previous record of 140 ka for better understanding the regional paleoclimate during previous glacials and interglacials. We address these issues in the following objectives:

(1) Determination of the timing of speleothem growth (i.e. periods of positive effective precipitation) during the last 550 ka using precise U–Th dating;
(2) Reconstruction of the origin of atmospheric precipitation using spatial speleothem growth patterns along the north–south transect, and their oxygen isotopic compositions;
(3) Interpretation of the vegetation types above the caves using carbon isotopic composition of the speleothems;

Using the regional pattern of speleothem deposition over several glacial–interglacials cycles, we aim to gain an understanding of the regional paleoclimate history of this part of northern Saharan-Arabian Desert with the context of global paleoclimate changes.

2. Geography, climate and geology of the Israeli deserts

2.1. Geographical definition, climatic zoning, geology and karst

Israel's present-day climate zoning is as follows: 1) Mediterranean climate (>350 mm of rainfall/year); 2) Mildly arid steppe/semi-desert (350–150 mm); 3) Arid/hyper-arid desert (<150 mm) (Fig. 1C). The Negev Desert is divided to three geographical regions (Fig. 1B and C): the mildly arid *northern Negev* forms a ~40 km wide belt between the ~350 mm and the ~150 mm isohyets, the arid *central Negev* (or *Negev Highlands*) has annual precipitation ranging from 150 mm in the north to 50 mm in the south and the hyper-arid *southern Negev* presently receives ~30–50 mm annual rainfall (Vaks et al., 2006) (Fig. 1C). Vegetation in the Negev Desert changes southward from C3 Mediterranean steppe forest at 350 mm isohyet to a mixture of C3 and C4 Irano-Turanian steppe and semi-desert in mildly arid and arid zones, and to Saharo-Arabian desert flora with high percentage of C4 plants in hyper-arid zone (Vogel et al., 1986; Danin, 1988; Goodfriend, 1990, 1999; Cerling and Quade, 1993; Feinbrun-Dothan and Danin, 1998).

Most exposed sedimentary rocks in the Negev are of Cretaceous–Pleistocene age. The karstic caves in the Negev mainly developed within dolomites and limestones of Cenomanian and Turonian age (Judea Group), with a few caves in Eocene limestone rocks (Suppl. Fig. 1, Suppl. Table 1).

2.2. Present-day regime of atmospheric precipitation in the Negev Desert

The northern and central Negev Desert receives most of its present-day rainfall during November to March from mid-latitude Atlantic-Mediterranean cyclones moving eastwards above the Eastern Mediterranean (EM) Sea (Dayan, 1986). Summers, between May and September, are hot and dry and result from the sinking air of sub-tropical highs, which develop over the Mediterranean Sea as strong high-pressure ridges pushed eastwards from the Azores Subtropical High Pressure Cell.

The EM Sea is the major moisture source for the precipitation. When passing over the land, the supply of moisture and latent heat becomes dramatically reduced to the south, and more gradually to the east (Shay-El and Alpert, 1991; Enzel et al., 2008). Thus, the northern Sinai coastline defines the southern limit at which rain clouds can form, and the latter are carried to the east by westerly winds, whereas the south remains dry (Zangvil and Druian, 1990). This results in a very sharp present-day rainfall gradient that decreases from central Israel toward the Negev Desert in the south (Fig. 1B and C).

Whereas northern Negev receives most winter precipitation from mid-latitude cyclones, the southern Negev receives its rainfall in sporadic short thunderstorms frequently associated with synoptic systems bringing moisture from the tropical Atlantic Ocean. These systems are common in the beginning and the end of the rainy season, approaching the region from the south-southwest (Kahana et al., 2002), and rarely affecting the northern Negev.

3. Methodology

3.1. Studied caves and sampling

Nine Negev Desert caves were studied (Fig. 1C, Suppl. Table 1): Hol-Zakh Cave (#1), Izzim Cave (#2), Makhtesh-ha-Qatan Cave (#3), Ashalim Cave (#4), Even-Sid mini-caves (#5), Ma'ale-ha-Meyshar Cave (#6), Wadi-Lotz Cave (#7), Shizafon mini-caves (#8), Ktora Cracks (#9), eight of these caves are located within Cretaceous (Cenomanian and Turonian) host dolomite and limestone and one within Eocene limestone. The coordinates and the characteristics of each cave are given in Suppl. Table 1. Thirty six speleothem samples were collected, including flowstones, stalactites, stalagmites and phreatic overgrowth calcite layers.

The speleothems vary in size from few mm thick flowstone crusts to ~40 cm long and ~20 cm thick stalagmites, stalactites, flowstones and phreatic overgrowth calcite layers. The samples were sectioned using a diamond saw to expose the internal structure and to identify and eliminate diagenetically altered samples (Bar-Matthews et al., 1997). Mineralogy and petrography was determined using petrographic microscope, Jeol 840 scanning electron microscope equipped with Oxford ISIS EDS system, and Philips PW 3020 X-ray diffractometer.

3.2. U–Th dating

U–Th dating analyses (123 samples representing growth layers from 31 speleothems from the nine caves) were performed using the MC-ICP-MS at the Geological Survey of Israel. Full analytical details are given in Suppl. Table 2. For the dating 10–800 mg calcite powder (depending on U concentration) was drilled using 0.8–4 mm diameter drill bits along the growth axis for stalagmites, and across the perpendicular cross section for stalactites and flowstones. A few layers were sampled in replicate by drilling at different points along the same layer (duplicate or triplicate dating is designated by the roman numerals I and II in Suppl. Table 2). The procedures for extraction and purification of U and Th as well as methodology of U–Th dating using MC-ICP-MS are described in detail by Vaks et al. (2006). U–Th ages were corrected for detrital ^{230}Th when ^{230}Th/^{232}Th activity ratio was <30 (Kaufman et al., 1998), assuming a ^{232}Th/^{238}U isotope atomic ratio of 4.25 in the detrital components (Lisker et al., 2010). Correction for the detrital component in speleothems with ^{230}Th/^{232}Th activity ratio >30 was not needed since the ages were within the error of the measured ages. Only seven speleothem layers needed such a correction. The limit of U–Th dating in this study is ~550 ka.

In order to determine the duration of speleothem growth, the top and bottom of each layers were dated. Where possible, several age determinations were made across a layer's cross section. Calculations of the growth rates during speleothem deposition were made with the assumption that the age represents the center of the drilled area, and that there is a constant growth rate between two dated points. Where layers were thinner than 4 mm only one U–Th age was measured and it was assumed that entire growth period of the layer was not longer than 1000 years, which is within the 2σ dating uncertainty. Such an assumption was also used when the ages at the top and the bottom of the layer were identical within analytical error.

3.3. Stable isotope analyses of speleothems and present-day rainwater

For δ^{18}O and δ^{13}C analyses, 1–2 mg samples were drilled using a 0.8 mm diameter drill, either along or across the growth axis. Hendy tests (14 measurements of δ^{18}O and δ^{13}C) were performed on stalactite ASH-11 (Ashalim Cave (#4)), flowstone HZ-1 (Hol-Zakh Cave (#1)) and stalagmite MMR-13 (Ma'ale-ha-Meyshar Cave (#6)) (Suppl. Fig. 2) to ensure that speleothem calcite deposition occurred in isotopic equilibrium with the dripping water (Hendy, 1971). All tested sampled were indicated to have deposited in equilibrium. 133 measurements of δ^{18}O and δ^{13}C were performed

on one stalagmite, five stalactites and five flowstone samples from caves at Hol-Zakh (#1), Makhtesh-ha-Qatan (#3), Ashalim (#4), Even-Sid (#5), Ma'ale-ha-Meyshar (#6) and Shizafon (#8), using VG SIRA-II Mass Spectrometer with ISOCARB system for carbonate analysis (Bar-Matthews et al., 1997). $\delta^{18}O$ and $\delta^{13}C$ values of calcite are reported in per-mil (‰) relative to the PDB standard. Because of the 0.8 mm size of the drill bits and the spacing between drilling points, $\delta^{18}O$ and $\delta^{13}C$ profiles were only possible on dated layers thicker than 4 mm. The isotope profiles and the U–Th ages allowed wiggle-matching of the profiles of different speleothems that grew during the same time period (from the same cave or the adjacent caves) within 2σ dating uncertainty of each sample.

Present-day rainfall samples were collected and the rainfall amounts and isotopic composition were measured during the two rainy seasons (from October to May) of 2004–2005 and 2005–2006, from five stations located on a north–south transect of the Negev Desert (Fig. 1C, Suppl. Table 3), Be'er-Sheva, Arad, Makhtesh-ha-Qatan (#3), Mitzpe-Ramon and Neot-Smadar. We also sampled the water from Ein-Netafim spring near Elat on the Gulf of Aqaba during June 2004, assuming that the spring water represents the average $\delta^{18}O$ and δD values of rainfall that fell in the several years preceding 2004.

In Be'er-Sheva and in Neot-Smadar each rain event was sampled during the winter of 2005–2006, whereas at the other sites rainwater was sampled at 20–45 days intervals after accumulating in plastic buckets with a 1 cm thick oil layer to prevent evaporation. The accumulated water samples were transferred to sealed plastic bottles and stored at +4 °C before analysis. This method was also applied in Neot-Smadar during the winter 2006–2007. $\delta^{18}O$ and δD measurements of the cave and rain waters were performed using methods described in Bar-Matthews et al. (1996) and Ayalon et al. (1998), and are reported in the SMOW scale. d-excess values are defined by the intercept in the local meteoric line equation: d-excess $= \delta D - 8 \times \delta^{18}O$.

4. Results

4.1. Petrography and field relations of the central and southern Negev speleothems

4.1.1. Vadose speleothems

Most speleothems formed in vadose (i.e. unsaturated) zone conditions, and consist of low-Mg calcite stalagmites, stalactites and flowstones. Based on field appearance, color, layer widths, and crystal size, the speleothems can be divided into three main stratigraphic members: Basal, Intermediate, and the outermost thin Young member. The Basal and Intermediate Members are older than 550 ka; they are massive and comprise >95% of the speleothem volume in the caves. Detailed descriptions of these speleothems are provided in Suppl. Fig. 3(1 and 2).

The Young member is 0.5–2 cm thick and composed of thinly laminated, columnar, low-Mg crystalline calcite. Precise dating of the uppermost 2–6 layers of this member was only possible at a few localities where the layers are thick enough (Section 4.2). The speleothem layers are composed of several mm thick light transmitting crystalline calcite layers separated by fine layers (<1 mm) of variably colored material (Suppl. Fig. 3(3)). The latter are composed of microcrystalline calcite, gypsum, halite, clays, quartz, and minor amounts of celestine, barite, apatite, and opaque minerals. The composition of the these fine layers is similar to the "patina" covering the surfaces of speleothems, suggesting that this material formed due to condensation corrosion (Auler and Smart, 2004; Dreybrodt et al., 2005), and/or to accumulation of evaporite or detrital minerals that were washed into the cave during rare rain events, and were left on speleothem surface upon drying.

4.1.2. Phreatic speleothems

Phreatic speleothems form in caves situated below the groundwater table and can be recognized as layers of calcite overgrowths covering the cave ceiling and walls, with no gravitational control on their morphology (Babic et al., 1996; Polyak and Asmerom, 2005). These speleothems are found in Makhtesh-ha-Qatan Cave (#3), the lowermost passages of Ashalim Cave (#4), Ma'ale-ha-Meyshar Cave (#6) and some small adjacent caves. The phreatic speleothems form 1–20 cm thick calcite overgrowth layers on the caves walls and ceilings (Suppl. Figs. 4A). They are older than 550 ka, except for Makhtesh-ha-Qatan Cave (#3), where a significant portion of these speleothems is younger. The latter grew in phreatic conditions during the early stages of their formation, whereas their younger outer layers grew in alternating phreatic/vadose conditions (Suppl. Fig. 4B).

4.2. U–Th ages and depositional periods of speleothems

The outermost layers of the Young member were dateable by U–Th method. Uranium concentrations mostly range between 0.04 ppm and ~2 ppm. High U concentrations (up to 10–20 ppm) characterize speleothems from Hol-Zakh (#1) and Ashalim (#4) caves, possibly because of their close location to overlying Senonian phosphorites, which contain ~120 ppm uranium (Soudry et al., 2002).

The dating results are presented in Fig. 2A and in Suppl. Table 2. They show that speleothem deposition was highly discontinuous. Intensities of speleothem deposition are shown using relative age frequency curve calculated using Isoplot/Ex3 software (Ludwig, 2003) (Fig. 2B, Suppl. Fig. 5-A–C). These graphs show that speleothem deposition clustered during the following intervals: 520–440 ka, 380–285 ka, 255–240 ka, 230–185 ka, 160–155 ka, 144–109 ka, and 89–86 ka. It should be noted that the 2σ age uncertainties for the 550–350 ka time interval are $> \pm 10$ ka and the precise duration of the speleothem deposition periods can not be determined. However, the calculation of the relative age frequencies shows that speleothem deposition almost ceased between 440 ka and 380 ka.

Speleothem deposition patterns during the last 350 ka fall into two groups (Fig. 2; Suppl. Fig. 5):

(1) *Intensive* deposition periods, defined by the measurement of at least two ages from two different caves. These periods occurred during three major time intervals: 350–290 ka, 220–190 ka, and 142–109 ka.
(2) Episodes with *limited* deposition as defined by a single age from one cave, occurring at 290–285 ka, ~247 ka, 225–220 ka, 190–185 ka, ~157 ka, 144–142 ka and ~88 ka.

Speleothems did not grow between 285 and 255 ka, 240 and 230 ka, 185 and 160 ka, 155 and 144 ka, 109 and 89 ka, 86 and 0 ka.

The frequency of depositional episodes decreases southwards; intensive speleothem deposition in the southern Negev only occurred between 350 ka and 310 ka, with limited deposition at ~138 ka. At 310–290 ka and 220–190 ka, when many speleothems formed in central Negev, there was no speleothem deposition in the south. Even-Sid mini-caves (#5) and Ma'ale-ha-Meyshar Cave (#6) are the southernmost locations of the 310–290 ka and 220–190 ka depositional periods, respectively.

Most ages follow stratigraphic order with the outermost layers being the youngest. However, there are age reversals in some layers adjacent to hiatuses or near the present-day surface, with the most prominent case being found in flowstone ASH-33 from the Ashalim Cave (#4) (Suppl. Table 2). The proximity of these layers to hiatuses suggests that secondary uranium mobilization processes could have

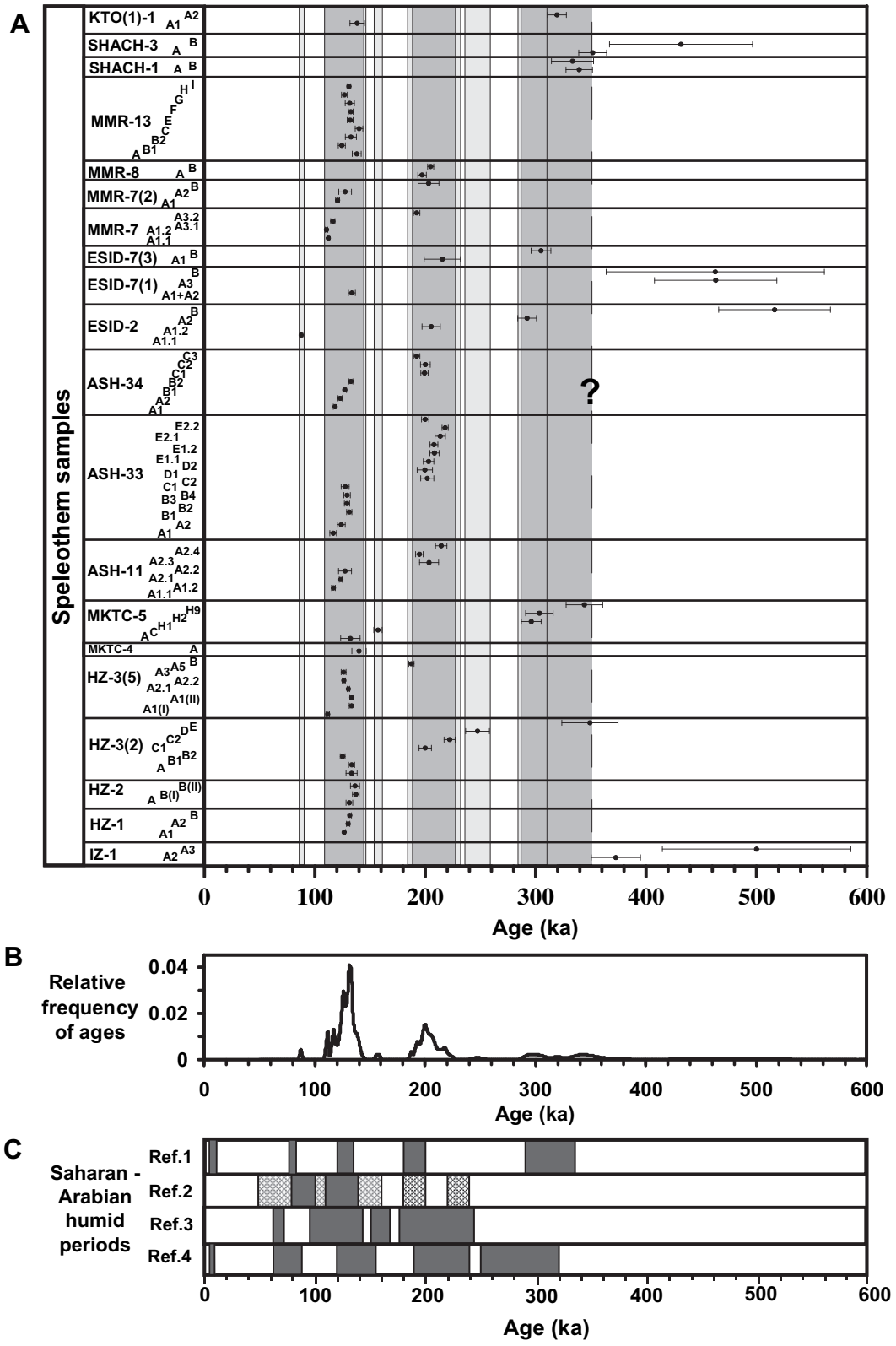

Fig. 2. Dating of central and southern Negev speleothems. A – Age distribution and periods of speleothem deposition of central and southern Negev Desert as determined by U–Th dating. The horizontal axis marks the age (ka), whereas the vertical shows the individual speleothems and their layers. Ages are marked as black circles with horizontal error bars. Vertical rectangles mark speleothem depositional periods: dark grey rectangles indicate periods of intensive speleothem deposition (two or more contemporaneous ages), light grey rectangles indicate periods of limited speleothem deposition (one age only). The 350 ka boundary of the speleothem deposition period between 350 ka and 310 ka is marked by question mark, because of the large uncertainties of the speleothem ages above 350 ka. (B) Relative frequencies of speleothem ages vs time. Age frequency is the fraction of speleothems deposited at a certain time with 95% confidence. (C) Timing of humid periods in southern Saharan-Arabian Desert (marked by rectangles) given on the same time scale as the periods of speleothem deposition in the Negev: Ref. 1 – Fleitmann et al. (2003); Ref. 2 – Osmond and Dabous (2004) (dark grey – most humid periods, light grey – less humid periods, white – dry periods); Ref. 3 – Crombie et al. (1997); Ref. 4 – Szabo et al. (1995).

occurred and/or secondary calcite was deposited. In some cases fragments of the host rock from the cave ceiling were identified which could have resulted in older age measurements (Suppl. Fig. 6).

4.3. Oxygen and carbon isotopic compositions of speleothems

4.3.1. Oxygen isotopic compositions

The composite isotopic records for each cave, based on the highest resolution record of each measured speleothem in cave, are presented in Fig. 3 and Suppl. Table 4A. (Isotopic records of few speleothems that are not included in composite records due to their lower resolution are shown in Suppl. Table 4B).

The oldest depositional episode dated to 516 ± 51 ka, shows high $\delta^{18}O$ values of −0.3‰ to −3.5‰ (Even-Sid Cave (#5), layer ESID-2-B), and possibly represents deposition during glacial MIS-14. $\delta^{18}O$ values for the 350–315 ka period (Shizafon mini-caves (#8)), range between −11.3‰ and −10.2‰ and are the lowest values found in the last 350 ka. From 305 ka to 285 ka (Makhtesh-ha-Qatan (#3) and Even-Sid (#5) caves) the $\delta^{18}O$ values vary between −4‰ and −1.6‰ (Fig. 3).

The deposition period occurred in the central Negev Desert between 230 ka and 185 ka, is represented by nine speleothems from 4 caves (Hol-Zakh (#1), Ashalim (#4), Even-Sid (#5) and Ma'ale-ha-Meyshar (#6)). However, an isotopic record could only be measured between 221 and 197 ka because other layers were too thin. $\delta^{18}O$ profiles for this period show variations between −6.9‰ and −10.5‰ (Fig. 3, Suppl. Table 4). Three sub periods can be defined from this record: from 221 to 219 ka the $\delta^{18}O$ values increase from −7.7‰ to −7.2‰; from 213 ka to 208 ka the $\delta^{18}O$ values decrease from −6.9‰ to −7.7‰ and between 208 ka and 197 ka $\delta^{18}O$ values decrease from −7.2‰ to −10.5‰. During a short speleothem deposition episode at ~157 ka the $\delta^{18}O$ values vary between −3‰ and −4.7‰ (Suppl. Table 4A).

The major speleothem deposition period in the central Negev Desert occurred between 144 ka and 109 ka, and is represented by fourteen speleothems from six caves. $\delta^{18}O$ profiles were measured on seven speleothems from caves Hol-Zakh (#1), Ashalim (#4), Even-Sid (#5) and Ma'ale-ha-Meyshar (#6), covering the time span from 133 ka to 115 ka. This time period can be divided into two isotopic sub periods: 133–127 ka, and 127–117 ka. During the first sub period $\delta^{18}O$ values oscillate between −7.9‰ and −10.2‰. The second period is marked by $\delta^{18}O$ differences between the two caves representing this interval. $\delta^{18}O$ values from Ashalim Cave (#4) vary between −7.4‰ and −8.5‰ from 127 ka to 118 ka, then sharply decrease to −9.8‰ at 117 ka, whereas $\delta^{18}O$ values from Ma'ale-ha-Meyshar Cave (#6) are almost constant, at −10.4‰ to −10.7‰ (Fig. 3).

The youngest period of speleothem deposition at 88–87 ka is characterized by $\delta^{18}O$ values between −7.7‰ and −8.1‰ (Fig. 3).

4.3.2. Carbon isotopic compositions

The composite isotopic profiles for each cave are given in Fig. 4 and Suppl. Table 4.

As with $\delta^{18}O$ values, significant $\delta^{13}C$ oscillations occur during speleothem depositional periods. Certain periods are characterized by relatively high ranges of $\delta^{13}C$ values: 516 ± 51 ka (−2.0‰ to −3.1‰, layer ESID-2-B), between 350 ka and 315 ka (+1‰ and −1.8‰), between 221 ka and 219 ka (+3.2‰ to +0.7‰, the highest values during the last 550 ka) and between 213 ka and 208 ka (from −0.2‰ to −0.6‰). Other periods are manifested in lower ranges of $\delta^{13}C$ values: between 305 ka and 285 ka (−3.2‰ to −7.5‰), between 208 ka and 197 ka (−0.5‰ to −6.8‰), at ~157 ka (−6‰ to −8.5‰), between 133 ka and 115 ka (−0.5‰ to −7.7‰), and at ~88 ka (−5.6‰ to −4.1‰).

4.4. Present-day rainfall in the Negev Desert: amounts and hydrogen and oxygen isotopic compositions

Amounts of annual rainfall and its $\delta^{18}O$ and δD values measured during 2004–2006 are given in Suppl. Table 3. Rainfall amounts decrease to the south and east: Be'er-Sheva, 207–389 mm; Arad, 53–161 mm; Makhtesh-ha-Qatan (#3), 25–122 mm; Mitzpe-Ramon, 48–50 mm; Neot-Smadar, 9–19 mm.

$\delta^{18}O$ of rainfall in the northern Negev (Be'er-Sheva, Arad) range between +6.4‰ and −11.8‰, and δD values vary between +37.4‰ and −68.3‰, (Fig. 5a; Suppl. Table 3). Weighted average $\delta^{18}O$ and δD values calculated as in Ayalon et al. (1998) are −4.7‰ and −17.6‰ respectively (d-excess = + 20.2‰) in Be'er-Sheva, and −4.1‰ and −13.8‰ (d-excess = + 19.1‰) in Arad (Fig. 5a; Suppl. Fig. 7).

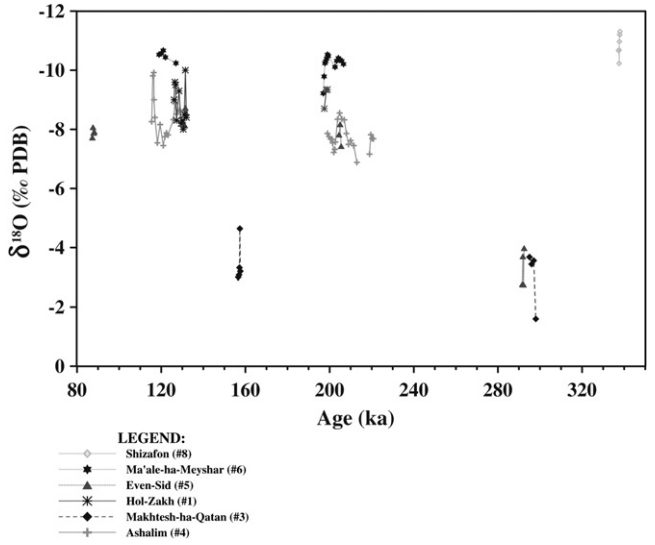

Fig. 3. Composite oxygen isotope profiles of central and southern Negev speleothems during the last 350 ka. In the legend the numbers of caves (as shown in Fig. 1) are given in brackets after the name of each cave.

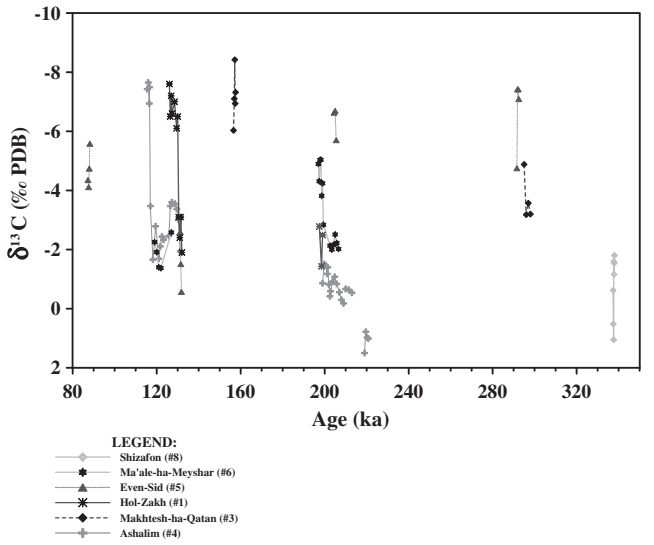

Fig. 4. Composite carbon isotope profiles of central and southern Negev speleothems during the last 350 ka. In the legend the numbers of caves (as shown in Fig. 1) are given in brackets after the name of each cave.

$\delta^{18}O$ of rainfall in the central and southern Negev vary between +5.1‰ and −8.0‰ and δD values range between +39.0‰ and −44.0‰ (Fig. 5b, Suppl. Table 3). All d-excess values lower than +1‰ are for rainfall events smaller than 2 mm. Weighed average rainfall $\delta^{18}O$ and δD values in Makhtesh-ha-Qatan (#3) for 2002–2006 are −2.4‰ and −6.1‰, respectively (d-excess = + 13.4‰, including results from Kuperman (2005) for 2002–2004); −3.3‰ and −11.1‰ (d-excess = + 15.1‰) in Mitzpe-Ramon, and −2.0‰ and −7.5‰ (d-excess = + 8.8‰) in Neot-Smadar (Suppl. Fig. 7). The average $\delta^{18}O$ and δD values of the Ein-Netafim spring water are −3.9‰ and −18.4‰ respectively, with d-excess of +13.2‰ (Suppl. Table 3).

5. Discussion

5.1. Humid episodes in central and southern Negev Desert

5.1.1. Speleothem deposition as recorder of effective precipitation

The terms "humid"/"wet" periods are used in this study to define episodes of speleothem deposition. During these intervals, the effective atmospheric precipitation during the rainy seasons was positive, sufficient available water for speleothem deposition enters the unsaturated zone, and the infiltration coefficient (the rainfall/snow fraction entering the groundwater) is greater than zero. Correspondingly, the term "arid/dry" defines periods without speleothem deposition, when the water entering the unsaturated zone is insufficient for speleothem growth, and the infiltration coefficient is zero.

In the present-day Mediterranean climate zone approximately ~1/3 of the annual rainfall reaches the unsaturated zone and the remaining 2/3 (about 300–350 mm in Soreq Cave area) is lost either by evaporation and/or by runoff (Ayalon et al., 1998, 2004). Nevertheless, the amount of water reaching the unsaturated zone is sufficient to allow continuous speleothem deposition today and was so throughout several glacial–interglacial episodes, including the entire Holocene (Bar-Matthews et al., 2003). The southernmost location of observed Holocene speleothem deposition is in Ma'ale-Dragot Caves, which are located close to the present-day 300 mm isohyet (Fig. 1C) (Vaks et al., 2006). No present-day speleothem deposition occurs in semi-desert and desert regions that receive less than ~300 mm of annual rainfall. Thus, the 300–350 mm isohyets can be defined as present-day limit of speleothem

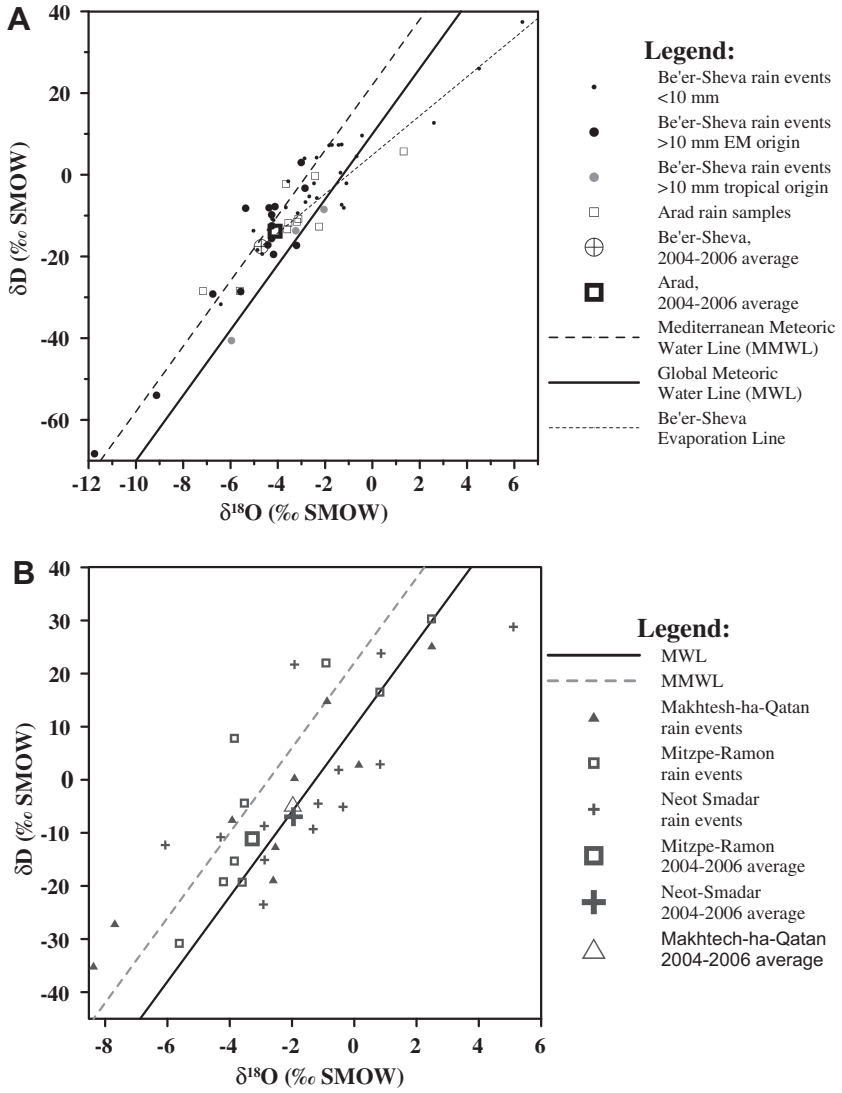

Fig. 5. (A) Oxygen and hydrogen isotopic composition of northern Negev rainfall during the years 2004–2006 including the data from Vaks et al. (2006). (B) Oxygen and hydrogen isotopic composition of the rainfall in central and southern Negev during the years 2004–2006 in Mitzpe-Ramon and Neot-Smadar, and during 2002–2006 in Makhtesh-ha-Qatan (#3) (including the data from Kuperman (2005)).

deposition in Israel; positive effective precipitation is located to the north of this boundary, and zero effective precipitation to its south.

During past interglacial periods, regional temperatures were similar to those of the Holocene, as shown by alkenone (Emeis et al., 1998, 2003), transfer function (Kallel et al., 2000), speleothem fluid inclusions (McGarry et al., 2004) and Δ_{47} ("clumped" isotopes) (Affek et al., 2008) temperatures. Thus we infer that at least 300–350 mm annual precipitation was required for the speleothem deposition in previous interglacials (Vaks et al., 2006).

During the glacial periods, regional temperatures were 3–10 °C lower than at present (Emeis et al., 2003; McGarry et al., 2004; Affek et al., 2008). According to the Clausius–Clapeyron relation cold air can hold less water vapor, leading to higher relative humidity. Indeed, during the last glacial the relative air humidity above the EM Sea was higher than at present (Affek et al., 2008). Relative humidity above the glacial Lake Lisan, the precursor of the Holocene Dead Sea, was ~0.9 (Kolodny et al., 2005), compared with 0.46–0.625 above present-day Dead Sea (Gat, 1984; Krumgalz et al., 2000). Since this, high humidity could lead to less evaporation of rain droplets and from soil surface, thus resulting in higher soil moisture and amounts of water infiltrating into the caves. Thus, a major question is what was the minimum precipitation necessary for speleothem deposition during the glacial periods?

At present, most infiltration to the unsaturated zone in northern and central Israel occurs during heavy mid-winter rainstorms when air temperature is below 10 °C. Negligible amounts of water reach the unsaturated zone when air temperature is >10 °C (Ayalon et al., 1998, 2004). To estimate what the infiltration coefficients could be in temperature conditions resembling the glacial conditions in Israel, we therefore used a data from a study from Dinaric karst area, Istria Peninsula, Croatia (Bonacci, 2001). In this area the annual precipitation is ~1000 mm and rain falls throughout the year. Bonacci's study showed that infiltration coefficients are 0.9–0.95 during the winter months when the average temperature is ~3.5 °C; i.e. that almost all the rain and snowmelt infiltrates to the aquifer. During April and October when average temperatures are 10 °C and 12 °C, respectively (similar to present-day average winter temperatures in Israel), the infiltration coefficients are ~0.6, and during the July and August when average temperature is ~21 °C, the infiltration coefficients drop to ~0.2. During years when most of the rainfall occurred during the hot season, the mean annual infiltration coefficient was 0.36, whereas in years where most of the precipitation fell in the cold season the mean coefficient was 0.76. The data of Bonacci (2001) thus suggest that the infiltration coefficients increase by ~50–60% when temperature drops from 10–12 °C to 3–4 °C. Based on this study we suggest that in the Mediterranean climate of Israel, an increase of ~50–60% in infiltration coefficients most probably would lead to a 75–100 mm reduction in the water loss due to evaporation/runoff during glacials. This implies a minimum amount of 200–275 mm annual precipitation (rainfall and snow) is required for speleothem deposition in glacial periods, compared to 300–350 mm today.

5.1.2. Humid periods in central and southern Negev Desert

Based on the numbers of ages and timing of speleothem deposition, as well as on the estimates for the minimum precipitation necessary for speleothem deposition during glacials and interglacials, we define the following rainfall/speleothem formation regimes during the last 350 ka in the central and southern Negev Desert. We correlate between these humid and arid episodes and the Marine Isotopic Stages (MIS) as defined by Shackleton and Opdyke (1973) and Martinson et al. (1987):

(1) Intensive speleothem deposition during interglacial periods reflecting humid events with annual precipitation exceeding 300 mm. These events occurred between 350 ka and 310 ka (interglacial MIS-9), between 220 and 190 ka (interglacial MIS-7.3, 7.2 and 7.1), and between 142 and 109 ka (including glacial MIS-6.1 – interglacial MIS-5.5 transition (Termination II), interglacial MIS-5.5, 5.4 and the beginning of MIS-5.3) (Fig. 2A and B; Suppl. Fig. 5).
(2) Intensive speleothem deposition during glacial periods, reflecting humid events with 200–275 mm (or more) of annual precipitation, represented by speleothem growth between 310 ka and 290 ka (glacial MIS-8.5) (Fig. 2A and B; Suppl. Fig. 5).
(3) Limited speleothem deposition during the interglacial periods where annual rainfall only rarely reached 300 mm. These episodes occurred at ~247 ka (transition from glacial MIS-8.1 to the interglacial MIS-7.5), 230–220 ka (transition from the MIS-7.4 to interglacial MIS-7.3), 190–185 ka (end of the interglacial MIS-7.1), and ~88 ka (transition from interglacial MIS-5.2 to MIS-5.1) (Fig. 2A and B).
(4) Limited speleothem deposition during glacial periods where annual precipitation did not exceed 200 mm, but conditions were more humid than at present. These humid events occurred between 290 ka and 285 ka (transition from glacial MIS-8.5 to MIS-8.4), at ~157 ka (glacial MIS-6.2) (Fig. 2A and B).
(5) Arid periods with no speleothem deposition occurred during the following periods: 285–255 ka, 240–230 ka, 185–160 ka, 155–144 ka, 109–89 ka, 86–0 ka.

Types (1) and (2) intensive rainfall regimes are defined here as "Negev Humid Periods" (NHP): NHP-4 from 350 ka to 310 ka; NHP-3 from 310 ka to 290 ka; NHP-2 from 220 ka to 190 ka, and NHP-1 – from 142 ka to 109 ka. During two older humid periods NHP-4 and NHP-3, the speleothem ages have large analytical errors. Their division is based on the fact that NHP-3 speleothem age frequency is the highest at ~295 ka, i.e. glacial MIS-8.5, whereas the NHP-4 age frequency is high at ~320 ka and ~342 ka, i.e. interglacial MIS-9 (Suppl. Fig. 5C). NHP-1, 2, and 4 are interglacials, but NHP-3 is glacial (MIS-8.5).

The existence of the six caves with speleothems dated for the NHP-1, the highest age frequencies and the relative thicker layers deposited during this period indicate that NHP-1 was the wettest during the last 350 ka. NHP-2 was also an important wet period, but conditions were slightly drier, as evidenced by the fact that speleothems from this period are found only in four caves and their age frequencies are lower. NHP-3 and 4 were drier, because their speleothems are found in fewer caves, their layers are thin, and age frequencies are low (Fig. 2A and B; Suppl. Fig. 5). NHP-4 was more intensive in the southern Negev and more limited in the central Negev. This contrasts with NHP-3, 2 and 1, which were most intense in the central Negev, but limited or absent in the southern Negev.

The thin layers of the Negev speleothems, alternating with hiatuses, suggest that each NHP represents clusters of short wet episodes with long droughts between them. The short durations of the wet episodes within each NHP accord with the absence of calcite horizons in the regolith soils of the southern Negev of Middle-Late Quaternary (Amit et al., 2006; Enzel et al., 2008).

5.2. Origin of rainfall in the Negev Desert

5.2.1. Present-day rainfall – eastern Mediterranean versus tropical sources

Precipitation from rain clouds forming above the EM Sea follows the local Mediterranean Meteoric Water Line (MMWL) ($\delta D = 8 \times \delta^{18}O + 22$) with an average d-excess of +22‰ (Gat and Carmi, 1987; Ayalon et al., 1998), compared to the global Meteoric Water Line (MWL) ($\delta D = 8 \times \delta^{18}O + 10$) (Craig, 1961). Maximum d-excess values exceed +40‰ (Bar-Matthews et al., 2003; Kuperman,

2005) also associated with EM moisture, whereas the d-excess in rainfall from tropical origin follows the MWL. Evaporation below the clouds decreases the d-excess in rain droplets, and their $\delta D - \delta^{18}O$ values form an "evaporation line" with a slope lower than 8, as found in present-day Jordan Valley rainfall (Vaks et al., 2003).

Most rain events in the northern Negev (Be'er-Sheva and Arad), have d-excess values between +16‰ and +34‰. The weighted mean isotopic compositions of Be'er-Sheva and Arad rainfall give d-excess values close to the MMWL (+20.2‰ and +19.4‰ respectively, (Fig. 5, Suppl. Fig. 7)). A small fraction of the rain events (mainly <10 mm) follow the MWL relationship, or fall on evaporation lines with d-excess values as low as −13‰. The lower d-excess values could represent an evaporated EM moisture source or rainfall of tropical origin. Synoptic system data from Israel Meteorological Service (http://www.ims.gov.il/) and the Skiron Forecasts of University of Athens (http://forecast.uoa.gr/forecastamg.html) indeed reveal that the three events with rain amounts >10 mm marked by grey circles on Fig. 5 were of tropical origin. Rain events at Be'er-Sheva station giving the most negative d-excess values (−8‰ to −13‰), define an evaporation line with an equation: $\delta D = 4.9 \times \delta^{18}O + 4.0$ (Fig. 5, Suppl. Fig. 7).

Rain events in the central and southern Negev Desert have d-excess values between +41‰ and −12.6‰ (Suppl. Table 2, Fig. 5), with averages of +15.1‰ in Mitzpe-Ramon, +13.4‰ in Makhtesh-ha-Qatan (#3) (this study and Kuperman (2005)), +8.8‰ in Neot-Smadar, and +13.2‰ in Ein-Netafim spring water near Elat. The average isotopic compositions of the rainfall in Mitzpe-Ramon, Makhtesh-ha-Qatan (#3) and Neot-Smadar lie on evaporation line for Be'er-Sheva rainfall (Suppl. Fig. 7). The available synoptic data (see previous paragraph) indicate that at Mitzpe-Ramon more than half of the rainfall originated in EM Sea, whereas in Makhtesh-ha-Qatan (#3) and in Neot-Smadar ~60% of the rainfall was from tropical origin. The d-excess value of +13.2‰ for Ein-Netafim spring water near Elat suggests mixing between EM and tropical origin rainfall.

Thus, the present-day Negev region and especially the central and southern parts receive rainfall of mixed tropical-EM Sea origin. This contrasts with central Israel, where almost all rainfall events are from the EM Sea source.

5.2.2. Origin of precipitation in the past – evidence from spatial trends in speleothem deposition

The speleothem deposition in arid and hyper-arid zones of the central and southern Negev occurred mainly during warmest interglacial periods. This contrasts with major periods of speleothem deposition in mildly arid semi-desert zones further to the north (northern Negev and Dead Sea/Jordan Valleys), where the major volume of speleothems was deposited during the glacial periods (although speleothem growth during the NHPs occurred there too) (Vaks et al., 2003, 2006; Lisker et al., 2010). Waldmann et al. (2010) suggest that this contrast was due to the different (i.e. southern) origin of atmospheric precipitation.

The thickness of speleothem cross sections (Fig. 6, Suppl. Fig. 8) and spatial pattern of speleothem deposition (Fig. 7) show a marked north to south decrease in their extent during the NHPs-1, 2 and 3 (Figs. 6 and 7, Suppl. Fig. 8). No speleothem deposition was found south of Ma'ale-ha-Meyshar Cave (#6) during NHP-2, and during NHP-3 no deposition occurred south of Even-Sid mini-caves (#5) (Fig. 7). During NHP-1 only a ~3 mm layer of speleothem was deposited in Ktora Cracks (#9) in southern Negev at ~138 ka, whereas in the central Negev the intensive deposition occurred from 142 to 109 ka and its thickness is more than 1.5 cm.

Thinning of speleothem cross sections from the north to the south is also evident on a larger scale of time and space. The height of largest stalagmites (from base to the top) in Soreq Cave exceeds 8 m, whereas in the northern Negev (Ma'ale-Dragot (MD), Tzavoa (TZ) and Izzim (#2) caves), the largest stalagmites are ~2–2.5 m in height. Further to the south large stalagmites are absent and the widest cross sections of stalagmites, flowstone and stalactites do not exceed 0.5 m.

These data clearly point to a north to south rainfall gradient reflecting rainout of the moisture source originating in the EM Sea. This gradient was present during NHP-1, 2 and 3, as well as during longer geological periods. Only during NHP-4 vadose speleothems were more common in southern Negev than in central Negev, possibly indicating an increased supply of moisture from the tropical source.

5.2.3. Origin of precipitation in the past – evidence from speleothem $\delta^{18}O$

Speleothems of the northern Negev show similar $\delta^{18}O$ trends to speleothems of central and northern Israel (Bar-Matthews et al., 2003; Vaks et al., 2006), and therefore provide further support that the EM Sea was the source of precipitation. In the central and southern Negev the difference between speleothem average $\delta^{18}O$ values during glacials (NHP-3) and during the interglacials (NHP-4, 2 and 1) is 5–5.5‰, which is similar or slightly greater than in northern parts of Israel. Thus, on the large time scale the EM Sea source does affect the precipitation to the region. However, the $\delta^{18}O$ profiles of speleothems deposited during NHP-2 and NHP-1 have different trends compared with speleothems from central and northern Israel and the northern Negev (Fig. 8). In particular, there is a marked difference in $\delta^{18}O$ trends at the transition from MIS-6.1 to MIS-5.5. In the Mediterranean climate region (Soreq Cave (SQ)) this transition occurs in three steps: at 140–139 ka, at 134–132.5 ka and at 128.5–127 ka, and the overall change is of ~−5.5‰ (Fig. 8). This change is partially seen in the northern Negev (Tzavoa cave (TZ) – Fig. 8), whereas there is a very little change in the speleothem $\delta^{18}O$ pattern during the MIS-6.1-MIS-5.5 transition in central and southern Negev, and there are much larger $\delta^{18}O$ oscillations (−7.5‰ and −10.5‰) between 127 ka and 121 ka. Whereas there is an increase by 2.5‰ in speleothem $\delta^{18}O$ after 121 ka in central Israel, in the Negev $\delta^{18}O$ values don't change significantly and become even more depleted after 118 ka. Additionally, there is an increase in speleothem $\delta^{18}O$ during peak of MIS-5.5 (128–120 ka) from the Negev to the north: central and northern Negev (−7.5‰ to −10.5‰); central Israel (−7‰ to −8.5‰); Peqi'in Cave in northern Israel (−7.7‰ to −6.2‰) (Bar-Matthews et al., 2003).

The different trends and the north–south decrease in speleothem $\delta^{18}O$ values could imply a different moisture source, for example a southern tropical source for the precipitation that affected the central and southern Negev. However, a significant southern source of atmospheric precipitation would have lead to considerable speleothem deposition in the southern Negev, whereas, as noted in previous section, speleothems show spatial decrease in their thickness from the north to the south during NHPs-1, 2 and 3. These isotopic trends are consistent with Rayleigh isotopic fractionation associated with increasing distance from the EM Sea coast (as suggested by Vaks et al. (2006) in the northern Negev).

$\delta^{18}O$ of present-day rainwater is usually isotopically heavy in the Negev compared to central and northern Israel. This is due to the low amounts of precipitation in the south, which cause evaporation below the clouds to be major factor controlling the higher $\delta^{18}O$ of the present-day rainfall (Vaks et al., 2003). This trend is the opposite of that expected for Rayleigh fractionation, which should lead to progressive isotopic depletion with rainout. However, Rayleigh fractionation is observed in central and northern Israel where the rainfall amounts exceed 350 mm (Bar-Matthews et al., 2003; Ayalon et al., 2004; Vaks et al., 2006). Thus, it is feasible that

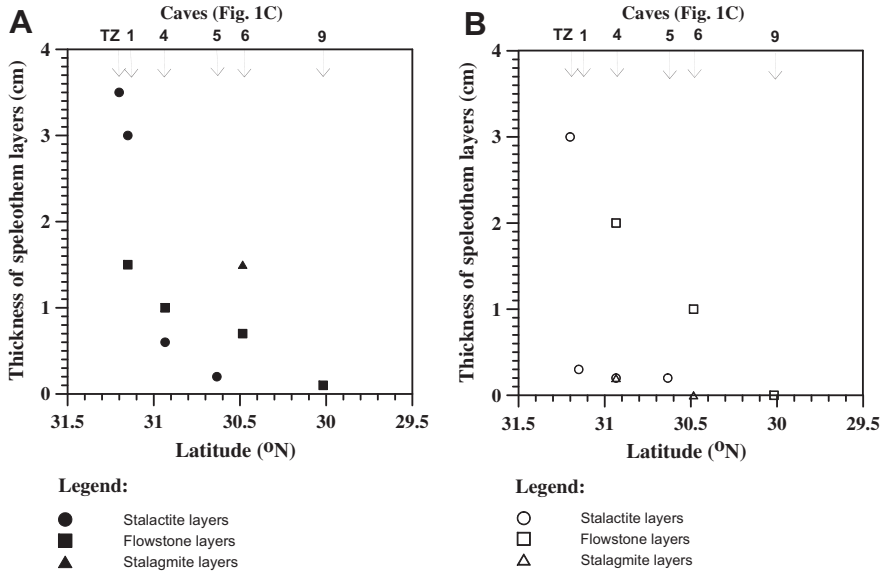

Fig. 6. Thinning of the speleothem layers from the north to the south in the Negev Desert during the NHP-1 (A) and during the NHP-2 (B). Caves are marked on the top horizontal axis with numbers as in Fig. 1 and with arrows pointing to the data points. "Layers" with thickness of 0 cm represent depositional hiatuses.

Rayleigh processes influenced the central and southern Negev during high rainfall periods (NHP 1–4), but not during the arid or hyper-arid periods like today.

The arguments presented above do not account for the contrast in speleothem deposition whereby speleothems in central and southern Negev were mainly interglacial, but glacial in the northern Negev. We suggest that during the glacial periods Atlantic-Mediterranean cyclones brought more than 200 mm/year of precipitation to the northern Negev (and Jordan/Dead Sea Valleys) for long periods, depositing thick speleothems. However, these glacial cyclones had moderate intensity and did not reach further to the south. During the NHPs the Atlantic-Mediterranean cyclones reached very high intensity reaching far to the south and bringing more than 300 mm to the central Negev (and more rarely

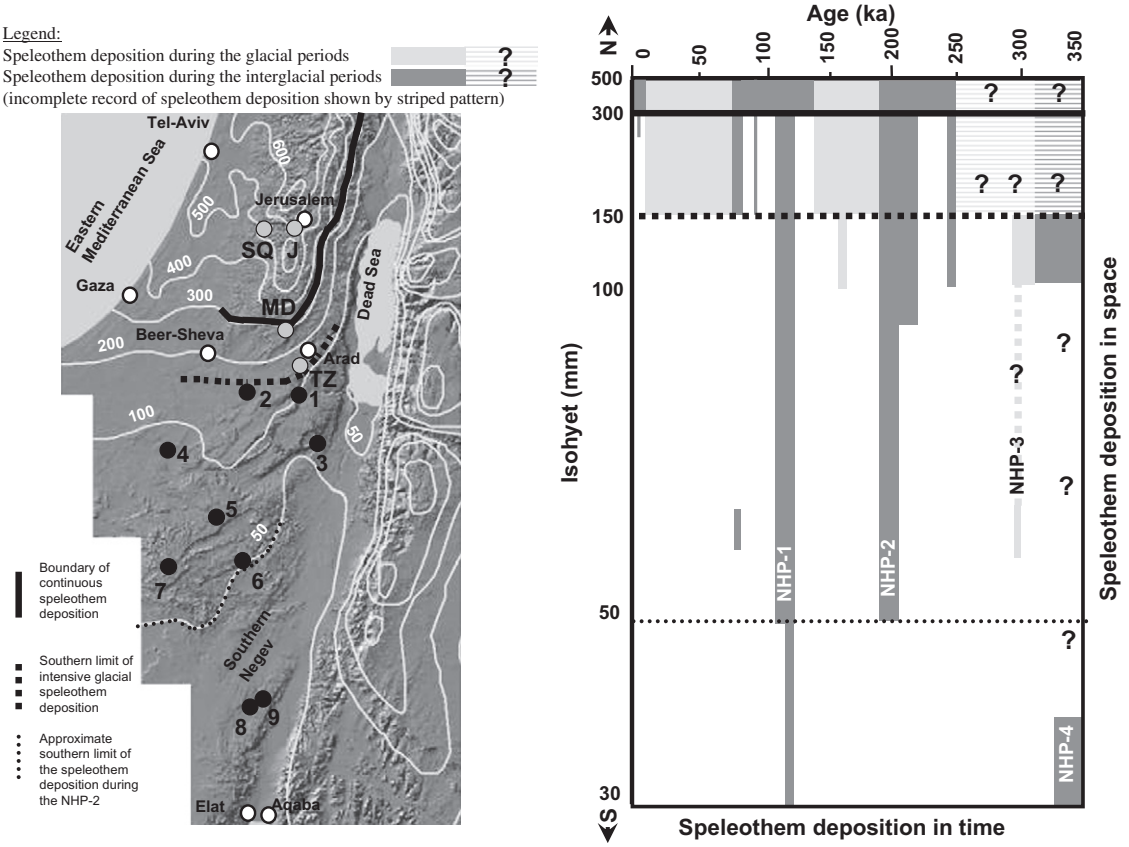

Fig. 7. Spatial distribution of the speleothem deposition in the Negev and central Israel showing the reduction of the speleothem deposition periods from the north to the south.

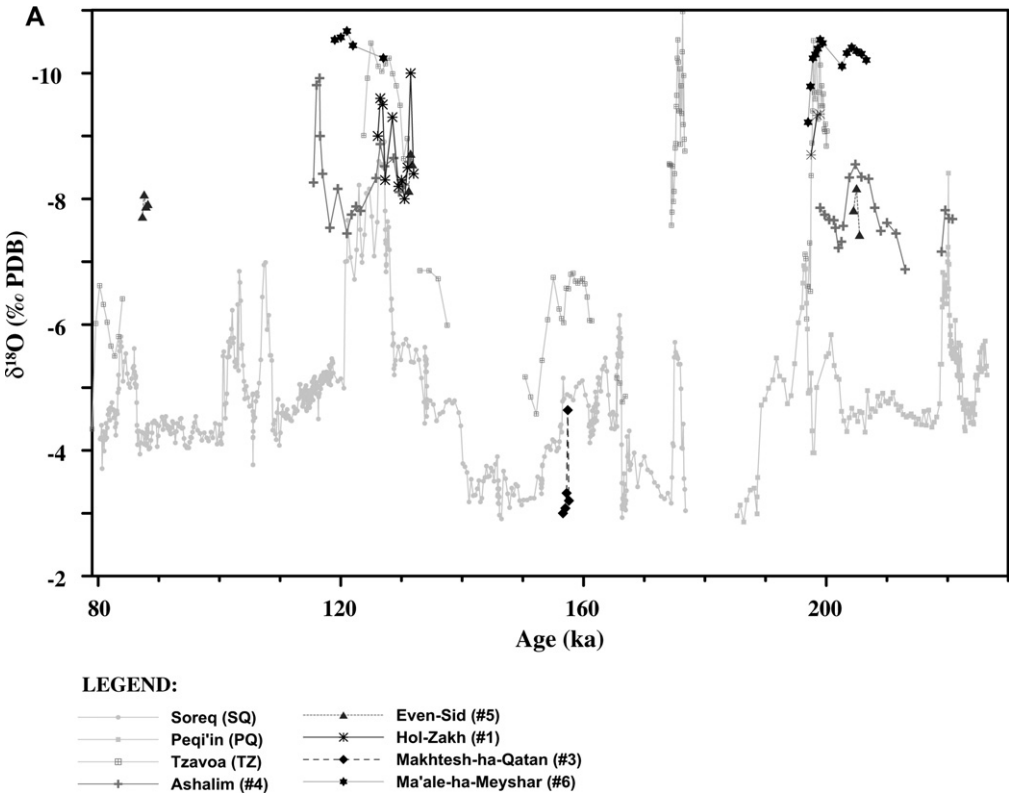

Fig. 8. $\delta^{18}O$ profiles of the central Negev speleothems compared with those of Tzavoa Cave, northern Negev and Soreq and Peqi'in Caves in central and northern Israel. In the legend abbreviations and numbers of the caves (as shown in Fig. 1) are given in brackets after the name of each cave.

to the southern Negev) in short-lived episodes, with the resultant deposition of thin speleothem layers.

5.3. Vegetation of the Negev Desert and its relation to climatic change

Speleothem $\delta^{13}C$ values in the central and southern Negev Desert vary between 1.5‰ and −8.4‰, and in most cases are much higher than those of the northern Negev (Vaks et al., 2006), Jordan Valley (Vaks et al., 2003), and central and northern Israel (Bar-Matthews et al., 2003) (Figs. 9 and 10, Suppl. Table 4). $\delta^{13}C$ values of speleothems from central and northern Israel reflect both the vegetation type and soil-water rock interaction (Bar-Matthews et al., 1996, 1997, 2003; Frumkin et al., 1999, 2000). $\delta^{13}C$ values ranging between −9‰ and −13‰ were interpreted to reflect C3 type vegetation and higher values during the last glacial were attributed to increase in the proportion of C4 type. $\delta^{13}C$ values range in the northern Negev from ~0‰ to −9.5‰ with an average of −6‰ (Vaks et al., 2006). The higher $\delta^{13}C$ values in the central and southern Negev (Figs. 9 and 10A) are considered to reflect the contributions of scarce C4 vegetation, host rock and atmospheric CO_2.

In most of the Negev speleothems, $\delta^{13}C$ values decrease from the beginning of the speleothem deposition episodes toward their end, thus indicating an increase in the surface vegetation cover above the caves. The lowest speleothem $\delta^{13}C$ values during NHP-2 and NHP-1 correlate well with high speleothem age frequencies at 208–197 ka, at 133–126 ka, and between 118 and 115 ka (Fig. 10A–C). This suggests that greater vegetation development occurred during the most intense rainfall periods. On the other hand, high speleothem $\delta^{13}C$ values at 220–208 ka (Ashalim Cave (#4)) and at 126–118 ka (Ashalim (#4) and Ma'ale-ha-Meyshar (#6) caves) associated with low speleothem age frequencies, suggest drier episodes during NHP-2 and 1 (Fig. 10A–C). The latter period, at the peak of MIS-5e, between 126 and 118 ka, is characterized by increased temperatures in central Israel and EM Sea (Ternois et al., 1997; Müller et al., 1998; Emeis et al., 2003; McGarry et al., 2004). It is thus possible that the increase in speleothem $\delta^{13}C$ in the central Negev between 126 and 118 ka reflects a reduction of vegetation cover as a result of increased evaporation and reduced soil moisture. This phenomenon did not occur in Tzavoa (TZ) cave further to the north, where $\delta^{13}C$ values decreased from 0‰ to −6‰ (Fig. 9), probably because it received higher rainfall.

In contrast to the decrease in $\delta^{13}C$ values in speleothems from the northern and central Negev between 205 ka and 197 ka and between 128 ka and 126 ka, sharp increases in speleothem $\delta^{13}C$ were found in Soreq, Jerusalem and Peqi'in caves from central and northern Israel (Fig. 9) (Frumkin et al., 1999; Bar-Matthews et al., 2003). Frumkin et al. (2000) interpreted the $\delta^{13}C$ increase in speleothem in Jerusalem cave between 128 and 121 ka to reflect aridification due to reduction in vegetation, forest fires and the stripping of the soil cover. However, this period corresponds to the formation of Mediterranean sapropel S5, which is considered by Kallel et al. (1997, 2000) to reflect increased precipitation over the entire Mediterranean Sea. The presence of deciduous oak pollen in the sapropel layers also indicates annual rainfall of >650 mm (Rossignol-Strick and Paterne, 1999). Bar-Matthews et al. (2000, 2003) therefore interpreted the increase in $\delta^{13}C$ values to reflect deluge events in central and northern Israel that resulted in fast water infiltration to the cave with little interaction with soil CO_2. This interpretation would better fit data indicating that rain in the Negev originated mainly from an EM Sea source (Section 5.2).

Speleothems that grew in the southern Negev during the NHP-4 in Shizafon mini-caves (#8) (~340–330 ka) are characterized by high $\delta^{13}C$ (−1.8‰–0.5‰) and very low $\delta^{18}O$ values (−11.3‰ to

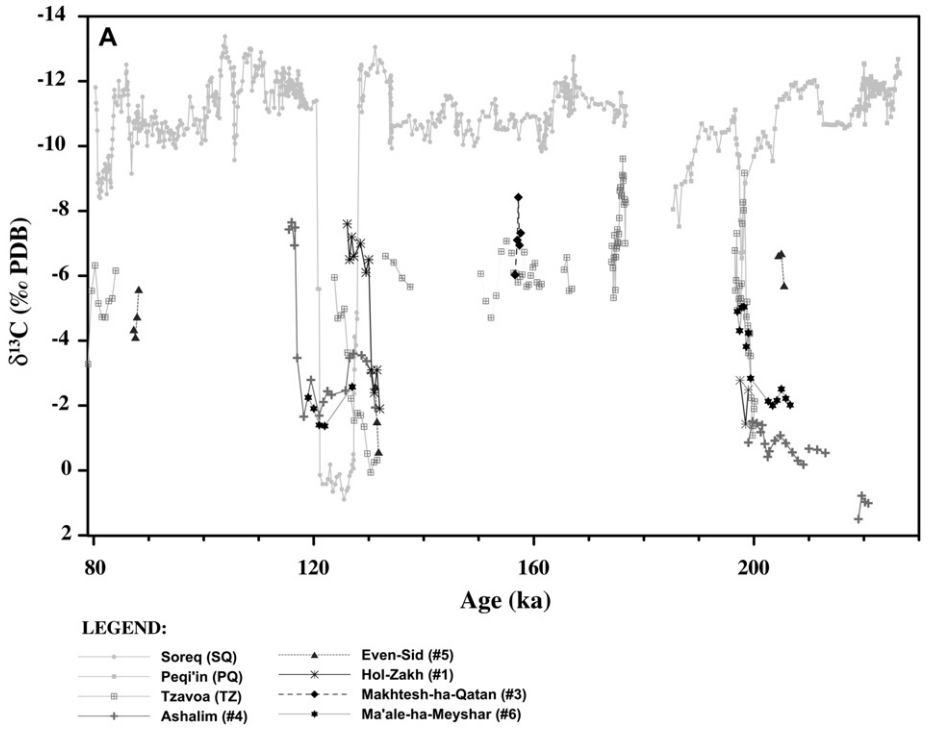

Fig. 9. $\delta^{13}C$ profiles of central Negev caves compared with those of Tzavoa Cave northern Negev, Soreq and Peqi'in Caves (central and northern Israel). In the legend abbreviations and numbers of the caves (as shown in Fig. 1) are given in brackets after the name of each cave.

−10.2‰). This indicates deposition during intense short wet episode and therefore that no significant vegetation development occurred above the caves.

Short episode of speleothem formation occurs in the central Negev in Makhtesh-ha-Qatan Cave (#3) at ~157 ka (glacial MIS-6.2), with $\delta^{13}C$ values of −8.4‰ (Figs. 9 and 10A). These are the lowest values measured for the central Negev speleothems. This speleothem is phreatic and during the MIS-6.2 the cave was probably located below the channel of wadi (Hazera). Thus the low $\delta^{13}C$ suggests that vegetation was locally developed in the wadi

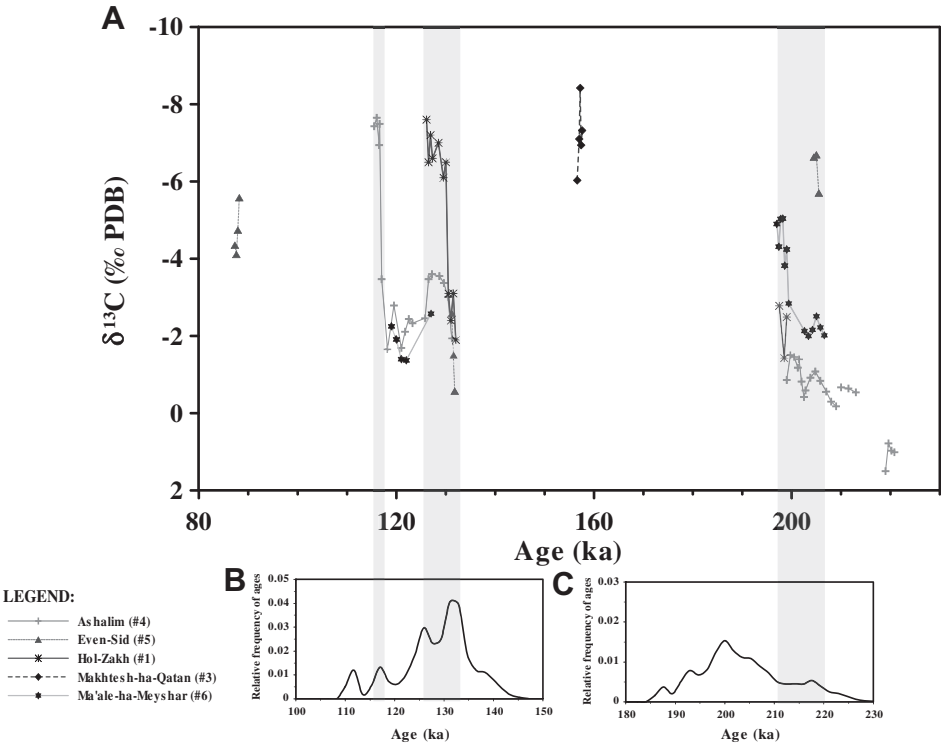

Fig. 10. $\delta^{13}C$ profiles of central Negev caves compared with relative frequencies of speleothem deposition in central and southern Negev (bottom) during NHP-1 (B) and NHP-2 (C). The grey rectangles show the highest relative frequencies of speleothem ages in the central and southern Negev.

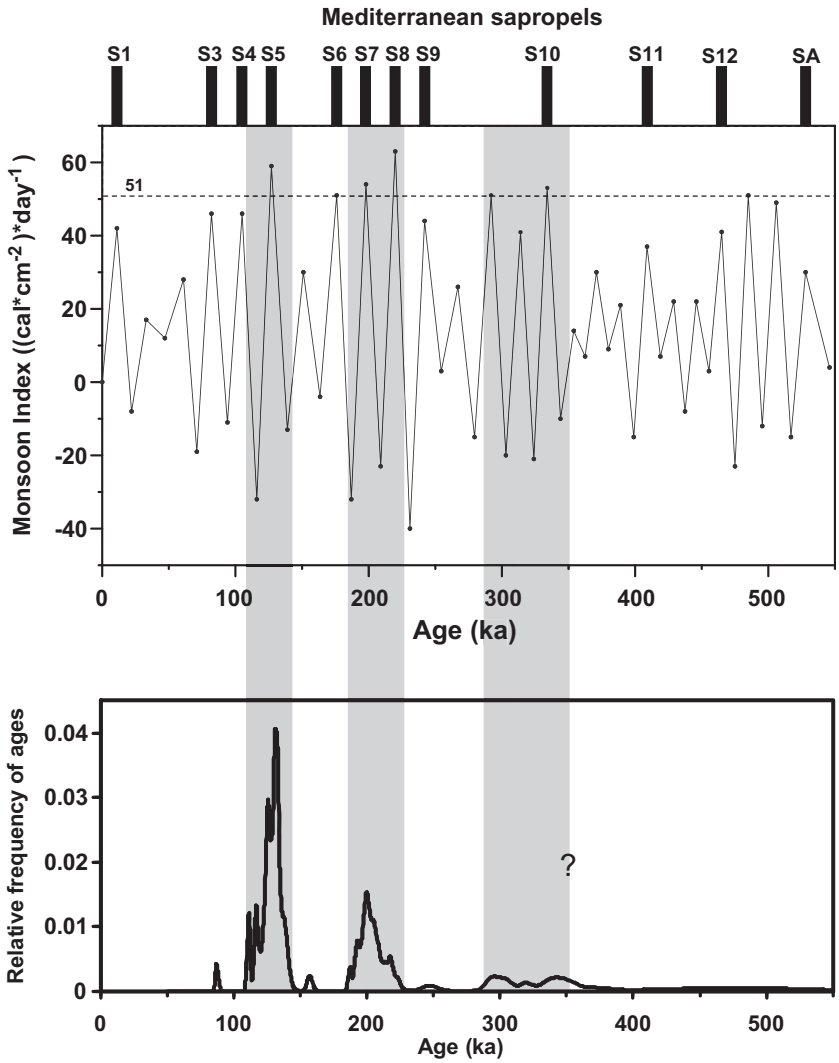

Fig. 11. Relative frequencies of the speleothem ages and NHPs (grey rectangles) compared with African monsoon index and timing of Mediterranean sapropels (Rossignol-Strick and Paterne, 1999). African monsoon index (M) in time (t) defined by Rossignol-Strick (1983) as: $Mt = I_T{}^t + (I_T{}^t - I_E{}^t)$, where I_T and I_E is insolation in units (cal × cm^{-2}) × day^{-1} at Tropic of Cancer and Equator, respectively. Fragmented horizontal line defines $Mt = 51$ (cal × cm^{-2}) × day^{-1}.

channel, or alternatively it may reflect a hypogene contribution which is not directly associated with surface vegetation. A deposition event in the central Negev between 89 and 86 ka gives $\delta^{13}C$ values = −4.2‰ to −5.6‰, suggesting dominant C4 semi-desert type vegetation.

5.4. Correlations between Negev Humid Periods, episodes of high African Monsoon Index and other regional/global climate changes

NHPs 4, 3, 2 and 1 in the central and southern Negev Desert coincide with periods of high amplitude oscillations in the solar energy in the northern and southern hemispheres (Berger, 1978) (Suppl. Fig. 9), peaks of northern Hemisphere insolation, an African monsoon index of ≥51 (cal × cm^{-2}) × day^{-1} (Rossignol-Strick, 1983) and the formation of the Mediterranean sapropels (Rossignol-Strick and Paterne, 1999) (Fig. 11).

NHP-4, 3, 2 and 1 are contemporaneous with speleothem deposition events that occurred in the Hoti Cave, northern Oman, at 330–300 ka, 200–180 ka, and 135–120 ka (Fig. 2C – Ref. 1). Fleitmann et al. (2003) suggested that Hoti cave deposition coincided with the northward migration of the ITCZ and intensification of the Indian Monsoon. Comparison between the timing of NHPs and humid periods from other parts of the southern Saharan-Arabian Desert, such as north-western Sudan and central and southern Egypt, shows that wet periods in the southern part of the Sahara Desert coincide with wetter conditions in the central and southern Negev (Fig. 2C, Refs. 2–4) (Szabo et al., 1995; Crombie et al., 1997; Osmond and Dabous, 2004); however the large age uncertainties of the former does not enable a precise correlation with NHPs.

Since this study suggests that the EM Sea probably was the major precipitation source to the Negev Desert, the link between maxima of the African monsoon and increased precipitation from Mediterranean sources may imply that the intensity of Atlantic-Mediterranean Cyclones must have increased contemporaneously with the African Monsoon. This was also suggested previously by Bar-Matthews et al., (2000, 2003) and Almogi-Labin et al. (2004) based on the timing of the anomalously low $\delta^{18}O$ and anomalously high $\delta^{13}C$ values of speleothems from the central and northern Israel. The most probable cause for the contemporaneous tropical and mid-latitude humid periods is that during higher northern hemisphere summer insolation periods, the SST in the sub-tropical Atlantic Ocean were higher, causing the Azorean high pressure cell to weaken, thus enabling intensive monsoon rainfall in the southern Sahara during the summer (deMenocal, 1995, 2004). The weaker

Azorean high pressure cell potentially leads to a more negative NAO index during winter, resulting in increased rainfall over the Mediterranean Sea (Hurrel, 1995; Krichak and Alpert, 2005) and ultimately above the Negev Desert. The absence of speleothems in the central and southern Negev Desert during the Holocene and probably during the MIS-11 (430–400 ka) could be explained by lower northern Hemisphere insolation, lower African Monsoon Index (Fig. 11), a stronger Azorean high pressure cell, and more positive winter NAO index, which prevented Atlantic-Mediterranean cyclones reaching their maximal strength, as during the NHPs.

Felis et al. (2004) used Sr/Ca ratios and $\delta^{18}O$ of annual aragonite bands in a 122 ka coral from Gulf of Elat (Aqaba) to show a water temperature summer–winter range of 8.4 °C, compared to 4.5–5.6 °C at present and during the Holocene. They argue that the increased seasonality probably arose from colder winters, and colder MIS-5.5 winters may be the result of a positive winter NAO index. However, Striem (1979) shows an opposite relation between mean winter temperatures in Israel and amounts of precipitation (i.e. colder winters are rainier). Krichak and Alpert (2005) show that decrease in precipitation in Israel during the last few decades is associated with positive NAO trend, whereas the rainy winters reflect a negative NAO index. Thus, we suggest that colder winter temperatures during NHP-1 indicate a negative rather than a positive NAO index, leading to increased winter precipitation.

It is still not clear what caused NHP events to commence several thousands years before the peaks of Northern Hemisphere insolation and the monsoon maxima, and to continue several thousands of years afterward. It is possible that the trigger of the NHPs is complex and not limited to the Northern Hemisphere. The sharp increase in speleothem age frequency at ~135 ka during the NHP-1 (Suppl. Fig. 5–A) coincides with the rise of the global sea level and global CO_2 (Henderson and Slowey, 2000; Gallup et al., 2002; Antonioli et al., 2004), which may be controlled by mechanisms in the Southern Hemisphere described by Broecker and Henderson (1998) and Stott et al. (2007). The start of the NHP-1 occurred the same time as the rapid warming in Italy (Drysdale et al., 2005, 2009) and in the Austrian Alps (Spotl et al., 2002), as well as the start of speleothem deposition in Oman (Fleitmann et al., 2003) and northern England (Baker et al., 1993).

5.5. Negev Humid Periods as climatic "windows" for hominid and animal dispersals from Africa

The Sinai-Negev land bridge was the major and probably the only route out of Africa before the early modern humans developed seafaring ability during the late Pleistocene (Derricourt, 2005). No other post-Miocene land bridges formed across the Red Sea (Fernandes et al., 2006), implying that wet climate conditions in "bottleneck" region of Sinai-Negev were of great importance for hominid and animal migrations during the Pleistocene. Vaks et al. (2007) and Osborne et al. (2008) show that NHP-1 humid episode in the Saharan-Arabian Desert could present an important impetus for early modern human migration from the African continent to the other parts of the world.

According to this and other studies (Szabo et al., 1995; Crombie et al., 1997; Fleitmann et al., 2003; Osmond and Dabous, 2004) humid conditions prevailed both in the northern and southern parts of Saharan-Arabian Desert between 200 ka and 195 ka (Fig. 2B and C), making the migration between central Africa through Sahara to the Levant easier. The major change from Acheulo-Yabrudian to early Mousterian tool industry in Levant occurred at ~200 ka (Barkai et al., 2003). Thus, NHP-1, NHP-2 and may be older humid periods could have played very important role by opening migration corridors and creating "climatic windows of opportunity" for the dispersion of hominids and animals out of the African continent.

6. Summary and conclusions

Speleothem deposition in present-day arid regions of Israel indicates that humid climatic conditions (i.e. periods with positive effective precipitation) occurred in the past.

During the last 350 ka major humid periods in the central and southern Negev Desert (Negev Humid Periods – NHP) occurred at 350–310 ka (NHP-4), 310–290 ka (NHP-3), 220–190 ka (NHP-2), and 142–109 ka (NHP-1). NHP-4, NHP-2 and NHP-1 occurred during interglacial periods (MIS-9, MIS-7 (1–3) and Termination II + MIS-5(5–4) respectively), whereas NHP-3 is associated with glacial period (MIS-8). Decrease in speleothem volume and width from the north to the south during the NHP-1, 2 and 3 indicates that the EM Sea was major source of atmospheric precipitation. Only during the NHP-4 the deposition of vadose speleothems in the southern Negev was more intensive than in the central Negev, and possibly reflects dominant tropical rain source. The decrease in speleothem $\delta^{13}C$ during the NHP-1 and 2 suggests that richer vegetation developed above the caves.

We estimate that a minimum of 200–275 mm/year was required for speleothem deposition during glacial periods, whereas during the interglacials 300–350 mm is required.

NHPs were contemporaneous with periods of monsoon index of $\geq$51 (cal/cm^2 × day) and formation of the sapropels in the Mediterranean Sea. Such simultaneous intensification of the monsoon and Atlantic-Mediterranean cyclones is probably related to the weakening of the high pressure cell above subtropical Atlantic Ocean, enabling the monsoon rainfall enter into southern and central Saharan-Arabian Desert during the summer and possibly decreasing the winter NAO index, causing the southern shift of Atlantic-Mediterranean cyclones. Although the maximum speleothem deposition during NHP-1 and 2 was contemporaneous with the maximum monsoon index, the start and the end of NHPs may be related to other type of climate forcing.

We suggest that NHPs occurring contemporaneously with the increased monsoon rainfall in southern Saharan-Arabian Desert could open climatic corridors for dispersals of hominids and animals out of the African continent.

Acknowledgments

This research was supported by the Israel Science Foundation (grant No. 910/05) and by the Ring Foundation. We would like to thank: A. Bein, B.Z. Begin, L. Halicz, N. Tepliakov, I. Segal, O. Yoffe, S. Ehrlich, A. Almogi-Labin, R. Amit, Y. Avni, S. Ashkenazi, B. Schilman, E. Eliani and M. Peri from Geological Survey of Israel for help in laboratory and field work, E. Vaks and E. Reznik-Vaks from Be'er-Sheva, Z. Wiener, N. Bloch and S. Bloch from Arad, G. Shenbrot from Ramon Science Center, and R. Dar from Neot-Smadar for the help with rainwater sampling; members of the Cave Research Unit at the Hebrew University Y. Yakobi, S. Lisker, R. Porat and A. Raikin for assistance with field work; the Israeli Nature and Parks Authority for permission to sample speleothems. We would also like to thank U. Dayan, Y. Enzel, L. Grossman, E. Hovers, N. Goren-Inbar from the Hebrew University. Special thanks to students U. Simchai, S. Leyzenbah, R. Kiro, S. Shlomi, N. Shalev, A. Wunsh, G. Garber and L. Laor for their help in laboratory and in the field.

Appendix. Supplementary information

Supplementary data associated with this article can be found, in the online version, at doi:10.1016/j.quascirev.2010.06.014.

References

Affek, H.P., Bar-Matthews, M., Ayalon, A., Matthews, A., Eiler, J.M., 2008. Glacial/interglacial temperature variations in Soreq cave speleothems as recorded by 'clumped isotope' thermometry. Geochimica et Cosmochimica Acta 72, 5351–5360.

Almogi-Labin, A., Bar-Matthews, M., Ayalon, A., 2004. Climate variability in the Levant and northeast Africa during the Late Quaternary based on marine and land records. In: Goren-Inbar, N., Speth, D. (Eds.), Human Paleoecology in the Levantine Corridor, pp. 117–134.

Amit, R., Enzel, Y., Sharon, D., 2006. Permanent Quaternary hyperaridity in the Negev, Israel, resulting from regional tectonics blocking Mediterranean frontal systems. Geology 34, 509–512.

Antonioli, F., Bard, E., Potter, E.-K., Silenzi, S., Improta, S., 2004. 215-ka history of sea level oscillations from marine and continental layers in Argentarola Cave speleothems (Italy). Global and Planetary Change 43, 57–78.

Auler, A.S., Smart, P.L., 2004. Rates of condensation corrosion in speleothems. Speleogenesis and Evolution of Karst Aquifers 2, 2 (4 pages).

Ayalon, A., Bar-Matthews, M., Sass, E., 1998. Rainfall-recharge relationships within a karstic terrain in the Eastern Mediterranean semi-arid region, Israel: [delta] ^{18}O and [delta] D characteristics. Journal of Hydrology 207, 18–31.

Ayalon, A., Bar-Matthews, M., Schilman, B., 2004. Rainfall Isotopic Characteristics at Various Cites in Israel and the Relationships with Unsaturated Zone Water. Israel Geological Survey, Report GSI/16/04, 37 pp.

Babic, L., Lackovic, D., Horvatincic, N., 1996. Meteoric phreatic speleothems and the development of cave stratigraphy: an example from Tounj Cave, Dinarides, Croatia. Quaternary Science Reviews 15, 1013–1022.

Baker, A., Smart, P.L., Ford, D.C., 1993. North-west European paleoclimate as indicated by growth frequency variations of secondary calcite deposits. Palaeogeography, Palaeoclimatology, Palaeoecology 100, 291–301.

Bar-Matthews, M., Ayalon, A., Matthews, A., Sass, E., Halicz, L., 1996. Carbon and oxygen isotope study of the active water–carbonate system in a karstic Mediterranean cave: implications for paleoclimate research in semiarid regions. Geochimica et Cosmochimica Acta 60, 337–347.

Bar-Matthews, M., Ayalon, A., Kaufman, A., 1997. Late Quaternary paleoclimate in the eastern Mediterranean region from stable isotope analysis of speleothems at Soreq cave, Israel. Quaternary Research 47, 155–168.

Bar-Matthews, M., Ayalon, A., Kaufman, A., 2000. Timing and hydrological conditions of Sapropel events in the Eastern Mediterranean, as evident from speleothems, Soreq cave, Israel. Chemical Geology 169, 145–156.

Bar-Matthews, M., Ayalon, A., Gilmour, M., Matthews, A., Hawkesworth, C.J., 2003. Sea-land oxygen isotopic relationships from planktonic foraminifera and speleothems in the Eastern Mediterranean region and their implication for paleorainfall during interglacial intervals. Geochimica et Cosmochimica Acta 67, 3181–3199.

Barkai, R., Gopher, A., Lauritzen, S.E., Frumkin, A., 2003. Uranium series dating from Qesem cave, Israel, and the end of the lower Paleolithic. Nature 423, 977–979.

Berger, A., 1978. Long-term variations of caloric insolation resulting from the Earth's orbital elements. Quaternary Research 9, 139–167.

Bonacci, O., 2001. Monthly and annual effective infiltration coefficients in Dinaric karst: example of the Gradole karst spring catchment. Hydrological Sciences-Journal-des Sciences Hydrologiques 46, 287–299.

Broecker, W.S., Henderson, G.M., 1998. The sequence of events surrounding Termination II and their implications for the cause of Glacial–Interglacial CO_2 changes. Paleoceanography 13, 352–364.

Cerling, T.E., Quade, J., 1993. Stable carbon and oxygen isotopes in soil carbonates, climate change in continental isotopic records. Geophysical Monograph 78, 217–231.

Craig, H., 1961. Isotopic variations in meteoric waters. Science 133, 1702–1703.

Crombie, M.K., Arvidson, R.E., Sturchio, N.C., El Alfy, Z., Zeid, K.A., 1997. Age and isotopic constraints on Pleistocene pluvial episodes in the western desert, Egypt. Palaeogeography, Palaeoclimatology, Palaeoecology 130, 337–355.

Danin, A., 1988. Flora and vegetation of Israel and adjacent areas. In: Yom-Tov, Y., Tchernov, E. (Eds.), The Zoogeography of Israel. Dr. W. Junk Publishers, Dordrecht, Netherlands.

Dayan, U., 1986. Climatology of Back Trajectories from Israel based on synoptic analysis. Journal of Climate and Applied Meteorology 25, 591–595.

Derricourt, R., 2005. Getting "Out of Africa": sea crossings, land crossings. Journal of World Prehistory 19, 119–132.

Dreybrodt, W., Gabrovšek, F., Perne, M., 2005. Condensation corrosion: a theoretical approach. Acta Carsologica 34, 317–348.

Drysdale, R.N., Zanchetta, G., Hellstrom, J.C., Fallick, A.E., 2005. Stalagmite evidence for the onset of the Last Interglacial in southern Europe at 129 ± 1 ka. Geophysical Research Letters 32, 1–4.

Drysdale, R.N., Hellstrom, J.C., Zanchetta, G., Fallick, A.E., Sanchez Goni, M.F., Couchoud, I., McDonald, J., Maas, R., Lohmann, G., Isola, I., 2009. Evidence for Obliquity forcing of glacial Termination II. Science 325, 1527–1531.

Emeis, K.C., Schulz, H.M., Struck, U., Sakamoto, T., Doose, H., Erlenkeuser, H., Howell, M., Kroon, D., Paterne, M., 1998. Stable isotope and alkenone temperature records of sapropels from sites 964 and 967: constraining the physical environment of sapropel formation in the eastern Mediterranean Sea. Proceedings of the Ocean Drilling Program, Scientific Results 160, 309–331.

Emeis, K.C., Schulz, H.M., Struck, U., Rossignol-Strick, M., Sakamoto, T., Erlenkeuser, H., Howell, M., Kroon, D., Mackensen, A., Ishizuka, S., Oba, T., Sakamoto, T., Koizumi, I., 2003. Eastern Mediterranean surface water temperatures and δ^{18}O composition during deposition of sapropels in the Late Quaternary. Paleoceanography 18, 1005. doi:10.1029/2000PA000617, 18 pp.

Enzel, Y., Amit, R., Dayan, U., Crouvi, O., Kahana, R., Ziv, B., Sharon, D., 2008. The climatic and physiographic controls of the eastern Mediterranean over the late Pleistocene climates in the southern Levant and its neighboring deserts. Global and Planetary Change 60, 165–192.

Feinbrun-Dothan, N., Danin, A., 1998. Analytical Flora of Eretz-Israel. CANA Publishing House Ltd, Jerusalem, Israel.

Felis, T., Lohmann, G., Kuhnert, H., Lorenz, S.J., Scholz, D., Patzold, J., Al-Rousan, S.A., Al-Moghrabi, S.M., 2004. Increased seasonality in Middle East temperatures during the Last Interglacial period. Nature 429, 164–168.

Fernandes, C.A.R., Rohling, E.J., Siddall, M., 2006. Absence of post-Miocene Red Sea land bridges: biogeographic implications. Journal of Biogeography 33, 961–966.

Fleitmann, D., Burns, S.J., Neff, U., Mangini, A., Matter, A., 2003. Changing moisture sources over the last 330,000 years in Northern Oman from fluid-inclusion evidence in speleothems. Quaternary Research 60, 223–232.

Frumkin, A., Ford, D.C., Schwarcz, H.P., 1999. Continental oxygen isotopic record of the last 170,000 Years in Jerusalem. Quaternary Research 51, 317–327.

Frumkin, A., Ford, D., Schwarcz, H., 2000. Paleoclimate and vegetation of the last glacial cycles in Jerusalem from a speleothem record. Global Biochemical Cycles 14, 863–870.

Gallup, C.D., Cheng, H., Taylor, F.W., Edwards, L.R., 2002. Direct determination of the timing of sea level change during Termination II. Science 295, 310–313.

Gat, J.R., 1984. The stable isotope composition of the Dead Sea waters. Earth and Planetary Science Letters 71, 361–376.

Gat, J.R., Carmi, I., 1987. Effect of climate changes on the precipitation patterns and isotopic composition of water in a climatic transition zone: case of the Eastern Mediterranean Sea area. In: The Influence of Climatic Change and Climatic Variability on the Hydrologic Regime and Water Resources, IANS 168 Symp. Proc., pp. 513–523.

Goodfriend, G.A., 1990. Rainfall in the Negev Desert during the middle Holocene, based on (super 13) C of organic matter in land snail shells. Quaternary Research 34, 186–197.

Goodfriend, G.A., 1999. Terrestrial stable isotope records of Late Quaternary paleoclimates in the eastern Mediterranean region. Quaternary Science Reviews 18, 501–513.

Hall, J., 1997. Digital Shaded-Relief Map of Israel and Environs, 1:500000. Israel Geological Survey.

Henderson, G.M., Slowey, N.C., 2000. Evidence from U–Th dating against Northern Hemisphere forcing of the penultimate deglaciation. Nature 404, 61–66.

Hendy, C.H., 1971. The isotopic geochemistry of speleothems-I. The calculation of the effects of different modes of formation on the isotopic composition of speleothems and their applicability as palaeoclimatic indicators. Geochimica et Cosmochimica Acta 35, 801–824.

Holmgren, K., Karlen, W., Shaw, P.A., 1995. Paleoclimatic significance of the stable isotopic composition and petrology of a late Pleistocene stalagmite from Botswana. Quaternary Research 43, 320–328.

Hurrel, J.W., 1995. Decadal trends in the north Atlantic oscillation: regional temperatures and precipitation. Science 269, 676–679.

Kahana, R., Ziv, B., Enzel, Y., Dayan, U., 2002. Synoptic climatology of major floods in the Negev Desert, Israel. International Journal of Climatology 22, 867–882.

Kallel, N., Paterne, M., Duplessy, J.C., Vergnaud-Grazzini, C., Pujol, C., Labeyrie, L., Arnold, M., Fontugne, M., Pierre, C., 1997. Enhanced rainfall on Mediterranean region during the last sapropel event. Oceanologica Acta 20, 697–712.

Kallel, N., Duplessy, J.C., Labeyrie, L., Fontugne, M., Paterne, M., Montacer, M., 2000. Mediterranean pluvial periods and sapropel formation over the last 200 000 years. Palaeogeography, Palaeoclimatology, Palaeoecology 157, 45–58.

Kaufman, A., Wasserburg, G.J., Porcelli, D., Bar-Matthews, M., Ayalon, A., Halicz, L., 1998. U–Th isotope systematics from the Soreq cave, Israel and climatic correlations. Earth and Planetary Science Letters 156, 141–155.

Kolodny, Y., Stein, M., Machlus, M., 2005. Sea-rain-lake relation in the last glacial east Mediterranean revealed by δ^{18}O–δ^{13}C in Lake Lisan aragonites. Geochimica et Cosmochimica Acta 69, 4045–4060.

Krichak, S.O., Alpert, P., 2005. Signatures of the NAO in the atmospheric circulation during wet winter months over the Mediterranean region. Theoretical and Applied Climatology 82, 27–39.

Krumgalz, B.S., Hecht, A., Starinsky, A., Katz, A., 2000. Termodynamic constraints of the Dead Sea evaporation: can the Dead Sea dry up? Chemical Geology 165, 1–11.

Kuperman, G. (2005). Reconstruction of Flood Periods by Dating Speleothems in Nahal Hazera, Northern Negev, Hebrew University of Jerusalem, M.Sc. Thesis (in Hebrew, English abstract).

Lisker, S., Vaks, A., Bar-Matthews, M., Porat, R., Frumkin, A., 2010. Late Pleistocene palaeoclimatic and palaeoenvironmental reconstruction of the Dead Sea area (Israel), based on speleothems and cave stromatolites. Quaternary Science Reviews 29, 1201–1211.

Ludwig, K.R., 2003. Isoplot 3.00, Special Publication No. 4. In: Ludwig, K.R. (Ed.), A Geochronological Toolkit for Microsoft Excel. Berkeley Geochronology Center, Berkeley CA 94709, USA 2455 Ridge Road.

Martinson, D.G., Pisias, N., Hays, J.D., Imbrie, J., Moore, T.C.J., Schackleton, N.J., 1987. Age dating and the orbital theory of the ice ages: development of the high-resolution 0–300,000 year chronostratigraphy. Quaternary Research 27, 1–29.

McGarry, S., Bar-Matthews, M., Matthews, A., Vaks, A., Schilman, B., Ayalon, A., 2004. Constraints on hydrological and paleotemperature variations in the

Eastern Mediterranean region in the last 140 ka given by the [delta] D values of speleothem fluid inclusions. Quaternary Science Reviews 23, 919–934.
Müller, P.J., Kirst, G., Ruhland, G., von Storch, I., Rosell-Mélé, A., 1998. Calibration of the alkenone paleotemperature index UK'37 based on core tops from the eastern South Atlantic and the global ocean (60N–60S). Geochimica et Cosmochimica Acta 62, 1757–1772.
Osborne, A.H., Vance, D., Rohling, E.J., Barton, N., Rogerson, M., Fello, N., 2008. A humid corridor across the Sahara for the migration of early modern humans out of Africa 120,000 years ago. PNAS 105, 16444–16447.
Osmond, J.K., Dabous, A.A., 2004. Timing and intensity of groundwater movement during Egyptian Sahara pluvial periods by U-series analysis of secondary U in ores and carbonates. Quaternary Research 61, 85–94.
deMenocal, P., 1995. Plio-Pleistocene African climate. Science 270, 53–59.
deMenocal, P.B., 2004. African climate change and faunal evolution during the Pliocene–Pleistocene. Earth and Planetary Science Letters 220, 3–24.
Polyak, V., Asmerom, Y., 2005. Orbital control of long term moisture in southwestern USA. Geophysical Reseach Letters 32, 1–4.
Rohling, E.J., Cane, T.R., Cooke, S., Sprovieri, M., Bouloubassi, I., Emeis, K.C., Schiebel, R., Kroon, D., Jorissen, F.J., Lorre, A., Kemp, A.E.S., 2002. African monsoon variability during the previous interglacial maximum. Earth and Planetary Science Letters 202, 61–75.
Rossignol-Strick, M., 1983. African monsoons, an immediate climate response to orbital insolation. Nature 304, 46–49.
Rossignol-Strick, M., Paterne, M., 1999. A synthetic pollen record of the eastern Mediterranean sapropels of the last 1 Ma: implications for the time-scale and formation of sapropels. Marine Geology 153, 221–237.
Schwarcz, H.P., 1986. Geochronology and isotopic geochemistry of speleothems. In: Fritz, P., Fontes, J.C. (Eds.), Handbook of Environmental Isotope Geochemistry. Elsevier, Amsterdam, pp. 271–300.
Shackleton, N.J., Opdyke, N.D., 1973. Oxygen isotopes and paleomagnetic stratigraphy of equatorial Pacific core V28–238: oxygen isotope temperatures and ice volumes on a 10^5 year and 10^6 year scale. Quaternary Research 3, 39–55.
Shay-El, Y., Alpert, P., 1991. A diagnostic study of winter diabatic heating in the Mediterranean in relation with cyclones. Quarterly Journal of Royal Meteorological Society 117, 715–747.
Soudry, D., Ehrlich, S., Yoffe, O., Nathan, Y., 2002. Uranium oxidation state and related variations in geochemistry of phosphorites from the Negev (southern Israel). Chemical Geology 189, 213–230.
Spotl, C., Mangini, A., Frank, N., Eichstadter, R., Burns, S.J., 2002. Start of the Last Interglacial period at 135 ka: evidence from a high Alpine speleothem. Geology 30, 815–818.
Stott, L., Timmermann, A., Thunell, R., 2007. Southern hemisphere and Deep-sea warming Led Deglacial atmospheric CO_2 rise and tropical warming. Science 318, 435–438.
Street, A.F., Grove, A.T., 1979. Global maps of lake-level fluctuations since 30,000 yr B.P. Quaternary Research 12, 83–118.
Striem, H.L., 1979. Some aspects of the relation between monthly temperatures and rainfall, and its use in evaluating earlier climates in the Middle East. Climatic Change 2, 69–74.
Szabo, B.J., Haynes, J.C.V., Maxwell, T.A., 1995. Ages of Quaternary pluvial episodes determined by uranium-series and radiocarbon dating of lacustrine deposits of Eastern Sahara. Palaeogeography, Palaeoclimatology, Palaeoecology 113, 227–242.
Ternois, Y., Sicre, M.-A., Boireau, A., Conte, M.H., Eglinton, G., 1997. Evaluation of long-chain alkenones as paleotemperature indicators in the Mediterranean Sea. Deep Sea Research, Part I 44, 271–286.
Vaks, A., Bar-Matthews, M., Ayalon, A., Schilman, B., Gilmour, M., Hawkesworth, C.J., Frumkin, A., Kaufman, A., Matthews, A., 2003. Paleoclimate reconstruction based on the timing of speleothem growth and oxygen and carbon isotope composition in a cave located in the rain shadow in Israel. Quaternary Research 59, 182–193.
Vaks, A., Bar-Matthews, M., Ayalon, A., Matthews, A., Frumkin, A., Dayan, U., Halicz, L., Almogi-Labin, A., Schilman, B., 2006. Paleoclimate and location of the border between Mediterranean climate region and the Saharo-Arabian Desert as revealed by speleothems from the northern Negev Desert, Israel. Earth and Planetary Science Letters 249, 384–399.
Vaks, A., Bar-Matthews, M., Ayalon, A., Matthews, A., Halicz, L., Frumkin, A., 2007. Desert speleothems reveal climatic window for African exodus of early modern humans. Geology 35, 831–834.
Vogel, J.C., Fuls, A., Danin, A., 1986. Geographical and environmental distribution of C3 and C4 grasses in Sinai, Negev, and Judean deserts. Oecologia 70, 258–265.
Waldmann, N., Torfstein, A., Stein, M., 2010. Northward intrusions of low- and mid-latitude storms across the Saharo-Arabian belt during past interglacials. Geology 38, 567–570.
Zangvil, A., Druian, P., 1990. Upper air trough axis orientation and the spatial distribution of rainfall over Israel. International Journal of Climatology IJCLEU 10, 57–62.